ORIGINAL RESEARCH

Deep RNA Sequencing Uncovers a Repertoire of Human Macrophage Long Intergenic Noncoding RNAs Modulated by Macrophage Activation and Associated With Cardiometabolic Diseases

Hanrui Zhang, MB, PhD*, Chenyi Xue, MS*, Ying Wang, MB, PhD*, Jianting Shi, MS; Xuan Zhang, PhD; Wenjun Li, BS; Sara Nunez, MS; Andrea S. Foulkes PhD; Jennie Lin, MD, MS; Christine C. Hinkle, MS; Wenli Yang, PhD; Edward E. Morrisey, PhD; Daniel J. Rader, MD; Mingyao Li, PhD; Muredach P. Reilly, MBBCh, MSCE

***Background*—**Sustained and dysfunctional macrophage activation promotes inflammatory cardiometabolic disorders, but the role of long intergenic noncoding RNA (lincRNA) in human macrophage activation and cardiometabolic disorders is poorly defined. Through transcriptomics, bioinformatics, and selective functional studies, we sought to elucidate the lincRNA landscape of human macrophages.

***Methods and Results*—**We used deep RNA sequencing to assemble the lincRNA transcriptome of human monocyte-derived macrophages at rest and following stimulation with lipopolysaccharide and IFN-γ (interferon γ) for M1 activation and IL-4 (interleukin 4) for M2 activation. Through de novo assembly, we identified 2766 macrophage lincRNAs, including 861 that were previously unannotated. The majority (≈85%) was nonsyntenic or was syntenic but not annotated as expressed in mouse. Many macrophage lincRNAs demonstrated tissue-enriched transcription patterns (21.5%) and enhancer-like chromatin signatures (60.9%). Macrophage activation, particularly to the M1 phenotype, markedly altered the lincRNA expression profiles, revealing 96 lincRNAs differentially expressed, suggesting potential roles in regulating macrophage inflammatory functions. A subset of lincRNAs overlapped genomewide association study loci for cardiometabolic disorders. MacORIS (macrophage-enriched obesity-associated lincRNA serving as a repressor of IFN-γ signaling), a macrophage-enriched lincRNA not expressed in mouse macrophages, harbors variants associated with central obesity. Knockdown of MacORIS, which is located in the cytoplasm, enhanced IFN-γ–induced JAK2 (Janus kinase 2) and STAT1 (signal transducer and activator of transcription 1) phosphorylation in THP-1 macrophages, suggesting a potential role as a repressor of IFN-γ signaling. Induced pluripotent stem cell–derived macrophages recapitulated the lincRNA transcriptome of human monocyte-derived macrophages and provided a high-fidelity model with which to study lincRNAs in human macrophage biology, particularly those not conserved in mouse.

***Conclusions*—**High-resolution transcriptomics identified lincRNAs that form part of the coordinated response during macrophage activation, including specific macrophage lincRNAs associated with human cardiometabolic disorders that modulate macrophage inflammatory functions. **(*J Am Heart Assoc*. 2017;6:e007431. DOI: 10.1161/JAHA.117.007431.)**

Key Words: genomics • induced pluripotent stem cells • inflammation • long noncoding RNA • macrophages

From the Division of Cardiology, Department of Medicine, Columbia University Medical Center, New York, NY (H.Z., C.X., Y.W., J.S., X.Z., M.P.R.); Cardiovascular Institute (W.L., C.C.H., E.E.M.), Department of Cell and Developmental Biology (E.E.M.), Division of Translational Medicine and Human Genetics, Departments of Genetics and Medicine (D.J.R.), Department of Biostatistics and Epidemiology (M.L.), and Department of Medicine (J.L.), Perelman School of Medicine, University of Pennsylvania, Philadelphia, PA; Department of Mathematics and Statistics, Mount Holyoke College, South Hadley, MA (S.N., A.S.F.); Institute for Regenerative Medicine, University of Pennsylvania, Philadelphia, PA (W.Y., E.E.M.); Irving Institute for Clinical and Translational Research, Columbia University, New York, NY (M.P.R.).

Accompanying Data S1, Tables S1 through S20, and Figures S1 through S7 are available at http://jaha.ahajournals.org/content/6/11/e007431/DC1/embed/inline-supplementary-material-1.pdf

*Hanrui Zhang, Chenyi Xue and Ying Wang contributed equally to this work.

The abstract of this article was presented at the American Heart Association Scientific Sessions, November 11–15, 2017, in Anaheim, CA.

Correspondence to: Hanrui Zhang, MB, PhD, Division of Cardiology, Department of Medicine, Columbia University Medical Center, 630 West 168th Street, PS10-401, New York, NY 10032. E-mail: hz2418@cumc.columbia.edu
Muredach P. Reilly, MBBCh, MSCE, Irving Institute for Clinical and Translational Research, Columbia University Medical Center, 622 West 168th Street, PH10-305, New York, NY 10032. E-mail: mpr2144@cumc.columbia.edu

Received August 17, 2017; accepted September 25, 2017.

Clinical Perspectives

What Is New?

- This study provides a comprehensive bioinformatic inventory of 2766 human macrophage long intergenic noncoding RNAs (lincRNAs).
- Subsets of macrophage lincRNAs overlap genetic variants for complex cardiometabolic disease traits and modulate macrophage inflammatory functions.
- Human induced pluripotent stem cell–derived macrophages recapitulate the lincRNA transcriptome of monocyte-derived macrophages and provide a high-fidelity model with which to study human macrophage lincRNAs, particularly those not conserved in mouse, in macrophage biology and diseases.

What Are the Clinical Implications?

- Among the 2766 human macrophage lincRNAs, 861 lincRNAs are newly annotated. Most (85%) are not syntenic or are not annotated as expressed in mouse, and many (21.5%) demonstrate tissue-enriched expression patterns, underscoring the importance of human lincRNA discovery studies, using deep RNA sequencing and de novo assembly, in a species- and tissue-specific manner.
- MacORIS (macrophage-enriched obesity-associated lincRNA serving as a repressor of IFN-γ [interferon γ] signaling) harbors variants associated with central obesity and functions as a brake on macrophage IFN-γ signaling, a very plausible mechanism for modulation of central obesity and related metabolic disorders.
- Targeting macrophage lincRNAs may have therapeutic potential in macrophage-related disorders in humans including metabolic disorders, atherosclerosis, and coronary artery diseases.

Long noncoding RNAs (lncRNAs), defined as >200 nucleotides in length and often 3′ polyadenylated,[1] are increasingly implicated in cardiovascular diseases.[2] Compared with mRNAs, lncRNAs are less abundant, mostly spliced but with fewer exons, and more species- and tissue-specific,[1,3] emphasizing the importance of studies on human- and cell-specific lncRNAs in human physiology and diseases.

As a critical component of the innate immune system, macrophages demonstrate remarkable plasticity and wide-ranging states of activation. Sustained and dysfunctional macrophage activation promotes inflammatory cardiometabolic diseases (CMDs) such as atherosclerosis and metabolic dysregulation.[4,5] Macrophage activation to M1 (classic inflammatory activation by lipopolysaccharide and IFN-γ [interferon γ]) and M2 (alternatively activated by IL-4 [interleukin 4]) phenotypes are well characterized in vitro models for study of human and murine macrophage biology.[6,7] Although the protein-coding transcriptome of human macrophages has been well characterized,[7–9] the lncRNA landscape in human macrophage biology remains elusive. Long intergenic noncoding RNAs (lincRNAs) lincRNA-Cox2[10] and lincRNA-EPS[11] have been shown to be critical regulators of inflammation in murine macrophages, but both lack human orthologs, limiting translational relevance to human. A handful of studies have mapped human macrophage lncRNAs, most using microarray[12–14] and THP-1 monocyte-derived macrophages (THP-1Φ),[12,13] yet THP-1Φ is karyotypically abnormal and immature and thus may differ from primary human macrophages.[15] Recent FANTOM5 (functional annotation of the mammalian genome) cap analysis of gene expression data sets have profiled transcription start site (TSS) and enhancer elements of lncRNAs in human monocyte-derived macrophages,[16,17] yet deep RNA sequencing (RNA-seq) of human macrophages has been lacking and is required to provide genomewide assembly of lncRNAs and to facilitate prioritization of promising lncRNAs for functional validation.

We have previously generated deep RNA-seq data sets of human peripheral blood mononuclear cell–derived macrophages (HMDMs)[18] with thorough characterization of their coding transcriptome[18] and alternative splicing events during M1 and M2 activation.[19] In this study, we focused on lincRNAs, a major subset of lncRNAs, using the same RNA-seq data sets.[18] LincRNAs do not overlap annotated protein-coding regions, facilitating experimental validation.[3] Because most genetic signals for complex traits are in intergenic regions, functional genetic variation in lincRNAs are likely to contribute to the intergenic genomewide association study (GWAS) signals for complex traits.[20] Through de novo transcriptome assembly, we (1) report a comprehensive lincRNA catalog (31% are newly annotated); (2) identify specific lincRNA expression patterns that correspond to distinct M1- and M2-activated phenotypes; (3) stratify macrophage lincRNAs based on synteny, conservation, tissue enrichment, and regulatory features defined by essential macrophage transcription factors (TFs) as well as histone H3 lysine 4 monomethylation (H3K4me1) and histone H3 lysine 4 trimethylation (H3K4me3) chromatin immunoprecipitation sequencing profiles[21,22]; (4) use GWAS data to identify macrophage lincRNAs related to human complex CMDs; (5) perform initial functional validation of MacORIS, a lincRNA that harbors single nucleotide polymorphisms (SNPs) associated with central obesity; and (6) characterize human induced pluripotent stem cell–derived macrophages (IPSDMs) as a model for functional assessment of human lincRNAs in macrophage biology. Our findings constitute a unique translational proof of principle and resource for the comprehensive interrogation of human macrophage lincRNAs in macrophage differentiation, inflammatory and metabolic functions, and relationship to human CMDs.

Methods

All human protocols for this work were approved by the University of Pennsylvania and Columbia University Medical Center human subjects research institutional review boards, and all participants provided written informed consent.

Human Macrophage Preparation, RNA-Seq Library Preparation, Sequencing, and Data Analysis

Human macrophage preparation, RNA-seq library preparation, sequencing, and data analysis were described previously[18] and in Data S1. Briefly, human peripheral blood mononuclear cells were differentiated to macrophages using 100 ng/mL macrophage colony-stimulating factor, and activation was induced by 18- to 20-hour incubation with 100 ng/mL lipopolysaccharide and 20 ng/mL IFN-γ for M1-like activation or 20 ng/mL IL-4 for M2-like activation.[18] Strand-specific, poly(A)+ libraries underwent deep sequencing at 100-bp paired-end reads to obtain in macrophages ≈130 million filtered reads per sample with >95% mapping rate[18] and in monocytes ≈280 million filtered reads per sample with >93% mapping rate.[23] RNA-seq reads were aligned with the hg19 reference genome, and transcript abundance was measured in FPKM (fragments per kilobase of transcript per million fragments mapped) using Cufflinks 2.1.1.[24] De novo assembly was performed using Cufflinks 2.1.1.[24] Differential expression, defined as false discovery rate–adjusted (FDR-adjusted) $P<0.01$ and a fold change >2, was tested with Cuffdiff. RNA-seq data are available under the accession number GSE55536.[18] (Table S1 shows participant demographics, and Figure S1 shows correlation between biological replicates). The bioinformatics pipeline for the annotation of the human macrophage lincRNA catalog, including the long intergenic transcript filters, coding potential filters and reliable expression filters, is outlined in Figure 1 and described in detail in Data S1.

Synteny and Conservation Analysis

Synteny is defined as conserved gene order along the chromosomes of different species. We examined the synteny of macrophage lincRNAs in mouse using HomoloGene release 68, then further subdivided syntenic lincRNAs as annotated or not annotated in mouse, using GENCODE M4 annotation. To evaluate sequence conservation for syntenic lincRNAs, the human lincRNA sequence was queried against the mouse genome with an E-value cutoff of 1×10^{-10} using BLASTN. Sequence hits in the mouse within the syntenic region were then searched in human samples with the same E-value cutoff. Sequences that passed the reciprocal steps were considered conserved.

Tissue Enrichment of lincRNA Expression

The fractional expression value of each lincRNA and mRNA was calculated by dividing the FPKM value in HMDMs by total FPKM values across HMDMs and 16 tissues from Human BodyMap RNA-seq data sets[3] (GSE30611).[25]

Histone Modification and Macrophage TF Profile Analysis

Histone H3 lysine 4 monomethylation (H3K4me1),[21,22] histone H3 lysine 4 trimethylation (H3K4me3),[21] histone H3 lysine 27 acetylation,[22] and PU.1 and C/EBPβ[22] chromatin immunoprecipitation sequencing data sets for human HMDM were downloaded from GSE31621[22] and GSE58310.[21] Data were quantified using computeMatrix from deepTools v1.5.11.[26]

Interrogation of Genomic Regions From GWAS

We first explored the overlap of macrophage-enriched lincRNAs with trait-associated SNPs that reached a significance level of $P<1\times10^{-5}$ using data from the comprehensive NHGRI (National Human Genome Research Institute) GWAS Catalog.[27] To further interrogate SNPs within macrophage lincRNAs for specific association with the 13 cardiometabolic traits (Table S2), 63 586 genotyped and imputed (HAPMAP[28]) SNPs were mapped to macrophage lincRNAs (±1 kb) and interrogated using either the minimum *P* value for the corresponding SNPs within each lincRNA (Bonferroni-adjusted threshold of $P<0.05$)[29] or a class-based method, GenCAT (Genetic Class Association Testing),[30] to test the overall impact of all SNPs within the region. Significantly associated lincRNAs were further prioritized to include only those that contained the strongest SNP-level *P* value in the region (±500 kb of the lincRNA) or if it was in low-linkage disequilibrium ($r^2<0.3$) with a stronger single SNP in the region, suggesting an independent signal at the lincRNA locus.

Validation, Characterization, and Initial Functional Studies of Candidate lincRNAs

Quantitative reverse transcriptase–polymerase chain reaction (qRT-PCR) was used to validate lincRNA expression, and primers are listed in Table S3. Knockdown of a top GWAS-associated lincRNA, MacORIS, was performed in THP-1Φ by transfection of single-stranded antisense oligonucleotides (Exiqon) and small interfering RNA (Dharmacon) using Lipofectamine RNAiMAX Transfection Reagent (Thermo Fisher Scientific). Western blotting was used to determine expression and phosphorylation of JAK2 (Janus kinase 2; Try1008) and STAT1 (signal transducer and activator of transcription 1;

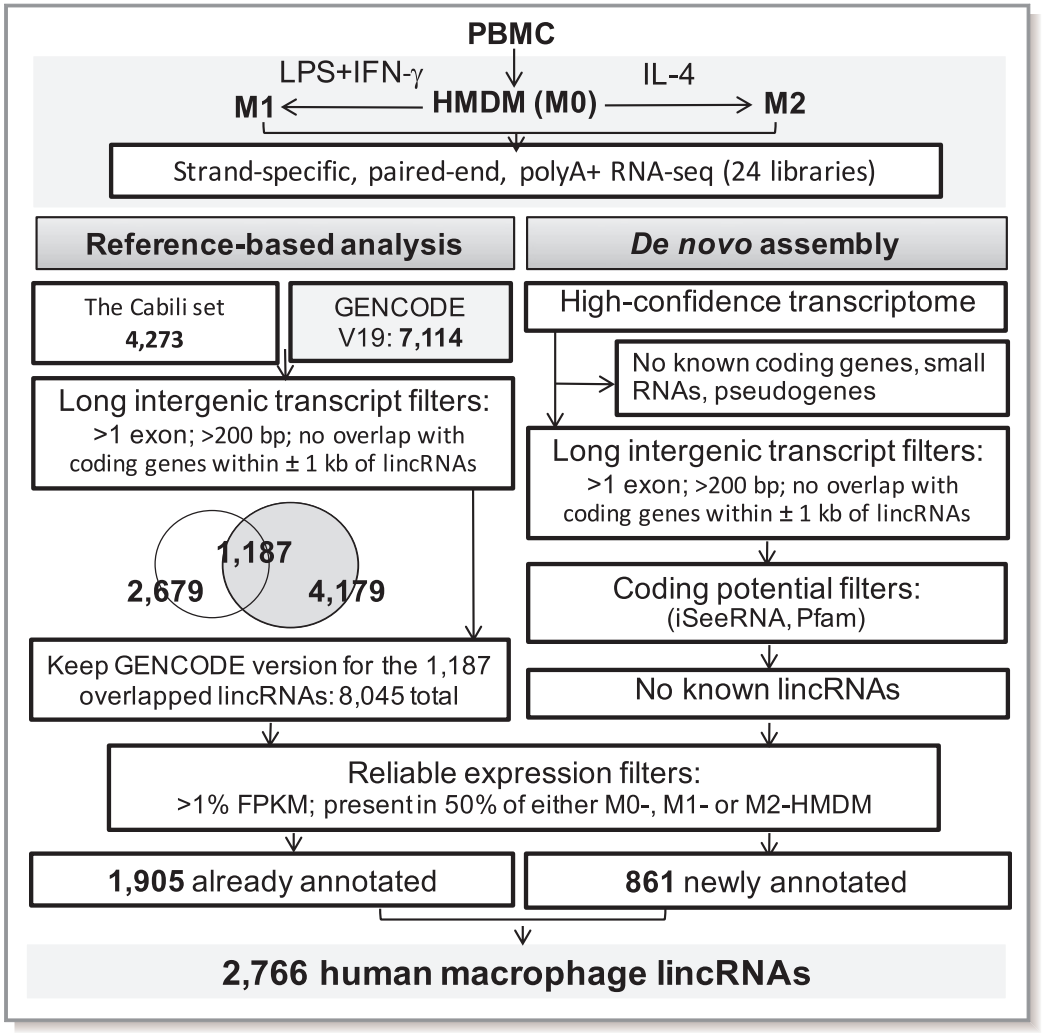

Figure 1. Global discovery of human macrophage lincRNAs. Polyadenylated RNA sequencing data generated from M0 HMDM and M1- or M2-activated HMDM were analyzed by the bioinformatics pipeline outlined for the annotation of known lincRNAs (the Cabili set and GENCODE V19) and newly annotated lincRNAs (from de novo assembly). FPKM indicates fragments per kilobase of transcript per million fragments mapped; HMDM, human peripheral blood mononuclear cell–derived macrophages; IFN-γ, interferon γ; IL-4, interleukin-4; lincRNA, long intergenic noncoding RNA; LPS, lipopolysaccharide; PBMC, peripheral blood mononuclear cells.

Tyr701). Flow cytometry was used to determine the expression of IFNGR1 (IFN-γ receptor 1).

Statistical Analyses

Specific analyses of RNA-seq and genomic data are described within each section. For analysis of gene ontology pathways in RNA-seq data, significant enrichment was declared at FDR-adjusted $P<0.05$ using the Benjamini and Hochberg method.[29] Nonsequencing data were analyzed with GraphPad Prism 6 (GraphPad Software). Differences between 2 groups were assessed by Student *t* tests (2-tailed). One-way ANOVA followed by the Dunnett test was used to correct for multiple comparisons. Results were declared significant if $P<0.05$.

Results

Whole-Transcriptome Profiling Identifies Previously Unannotated Human Macrophage lincRNAs

We interrogated a stringent set of known multiexon human lincRNAs (>200 bp, no overlap with a protein-coding gene within ±1 kb of lincRNAs) collated from (1) the "Cabili" Human BodyMap "stringent" data set (4273 lincRNAs)[3] and (2) the GENCODE V19 data set (7114 lincRNAs; Figure 1).[31] By combining the 2 sets, a catalog of 8045 known multiexon lincRNAs was generated. Next, we performed de novo transcriptome assembly by Cufflinks v2.1.1 and excluded previously annotated multiexon lincRNAs, as described in

Data S1. We filtered single-exon lincRNAs because of greater probability of transcriptional noise.[32] We applied a coding potential filter on newly annotated lincRNAs using iSeeRNA[33] and HMMER-3 on Pfam[34] (Figure 1). To identify lincRNAs that were robustly and reliably expressed in human macrophages, we included only lincRNAs expressed at >1% FPKM based on FPKMs for all lincRNAs and mRNAs in at least 50% of subjects in all HMDM samples. Through this conservative, multilayered analysis, we identified 2766 distinct multiexon lincRNAs that are reliably expressed in human macrophages, of which 861 were previously unannotated (Figure 1). Coding potential for all 2766 lincRNAs was further validated by PhyloCSF,[35] as described in Data S1, and the lincRNAs with scores higher than the threshold cutoff were listed in Table S4.

Among the 2766 lincRNAs, 1282 lincRNAs were found in all 6 M0, M1, or M2 HMDMs, and 562 lincRNAs were expressed in all 18 unique macrophage samples (Table S5). More than 50% (1407) of lincRNAs were found across all M0-, M1-, and M2-HMDM activation states, whereas a smaller portion of lincRNAs were highly specific to M0, M1, or M2 HMDMs (Figure S2A). These latter "activation state"–specific lincRNAs were more likely to be previously unannotated lincRNAs (Figure S2B and S2C), underscoring the importance of interrogating lincRNAs within cell-specific and functional contexts.

Expression and Conservation of Macrophage lincRNAs

As in other cell types,[3] compared with protein-coding genes, macrophage lincRNAs were generally expressed with less abundance, were shorter, and had fewer exons than mRNAs (Figure 2A and Figure S3). Expression levels of newly annotated macrophage lincRNAs were lower than those of known lincRNAs (Kolmogorov–Smirnov test, $P<2.2\times10^{-16}$; Figure 2A).

The majority of human macrophage lincRNAs are not conserved in mouse

Many functional lincRNAs are suggested to have synteny (genomic regions flanked by homologous protein-coding genes)[1] despite low sequence similarity across species.[36] Of the 2766 macrophage-expressed lincRNAs, 61% (1678) were syntenic, yet only 400 of these 1678 lincRNAs were annotated as expressed in mouse GENCODE M4. At this time, ≈85% (2366) of human macrophage lincRNAs are nonsyntenic or are syntenic but not expressed in mouse

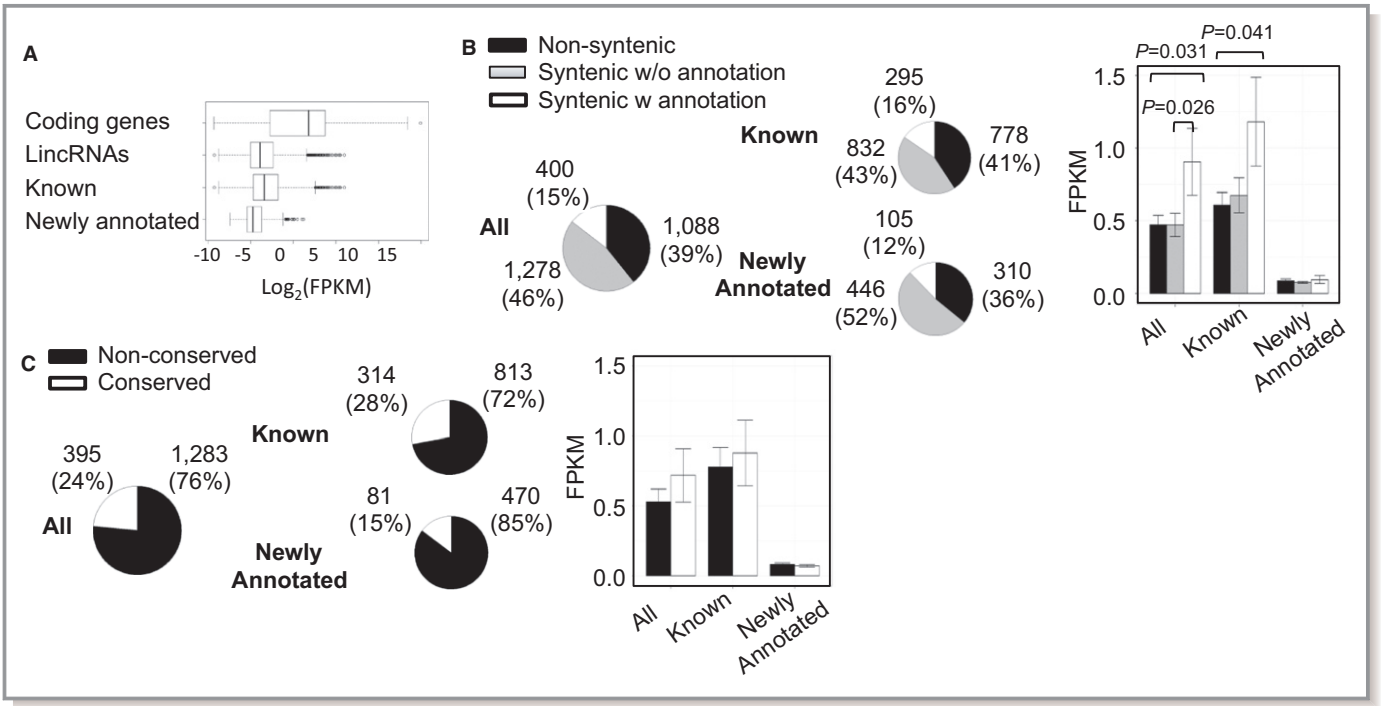

Figure 2. Expression, synteny, and conservation of macrophage lincRNAs. A, Expression measured as FPKM for gene categories. The lincRNAs had overall lower expression than coding genes. B, Most lincRNAs were nonsyntenic or were syntenic but not annotated as expressed in mouse. Compared with known lincRNAs, newly annotated lincRNAs showed lower percentages of synteny and annotation in mouse. The lincRNAs that were syntenic and annotated in mouse showed higher expression than other lincRNAs. C, The lincRNA sequence conservation between human and mouse in syntenic regions was examined using BLASTN (see Methods). The lincRNAs demonstrated poor sequence conservation in the syntenic regions, and newly annotated lincRNAs were less conserved than known ones. FPKM indicates fragments per kilobase of transcript per million fragments mapped; lincRNA, long intergenic noncoding RNA.

(Figure 2B). Among the 1678 syntenic lincRNAs, only 24% (395) demonstrated significant sequence conservation (Figure 2C) between human and mouse.[37] Compared with previously known lincRNAs, a lower proportion of newly annotated macrophage lincRNAs was conserved (28% versus 15%, respectively; $P=3.49\times10^{-9}$), suggesting a higher level of species specificity (Figure 2C). Although lincRNAs that were syntenic and annotated as expressed in mouse showed higher expression in human macrophages than other lincRNAs (Figure 2B), sequence conservation per se was not associated with expression levels in human macrophage (Figure 2C).

Tissue Enrichment and TF Profiles of Macrophage lincRNAs

Enrichment of lincRNAs in macrophages, relative to other tissues, may suggest their specific roles in macrophage biology. Consequently, we determined the tissue enrichment of macrophage lincRNAs by calculating their expression in macrophages relative to the sum of expression across 16 tissues in data from the Human BodyMap RNA-seq.[3] Applying a fractional expression of >0.2 to define "enriched" lincRNAs,[3] 595 lincRNAs within the 2766 macrophage lincRNAs (21.5%) demonstrated enriched expression in HMDMs (Table S5). Relative to protein-coding genes, macrophage lincRNAs were proportionally more macrophage enriched (eg, 15.3% versus 9.8% in M0 HMDM; Figure 3A). Certain lincRNAs were specifically enriched only in M1 or M2 HMDM (Figure 3B, Table S5). Expression levels of macrophage-enriched lincRNAs were higher than those of nonenriched lincRNAs (Figure 3C).

PU.1 and C/EBPβ are essential TF regulators of macrophage differentiation.[22] Leveraging public data sets (GSE31621),[22] we discovered that TF occupancy was significantly higher around (±2 kb) lincRNA TSS and gene bodies for macrophage-enriched lincRNAs than for non–macrophage-enriched lincRNAs; indeed, the majority of the enriched lincRNAs demonstrated PU.1 or C/EBPβ binding (Figure 3D). In comparing M0 HMDM to our human monocyte data (RNA-seq of 6 age- and race-matched subjects[23]; Table S1), numerous lincRNAs were differentially expressed (DE; fold change >2 and FDR <0.01) during monocyte transition to HMDM (Figure S4A and S4B and Table S6); many of the upregulated lincRNAs harbored PU.1 and

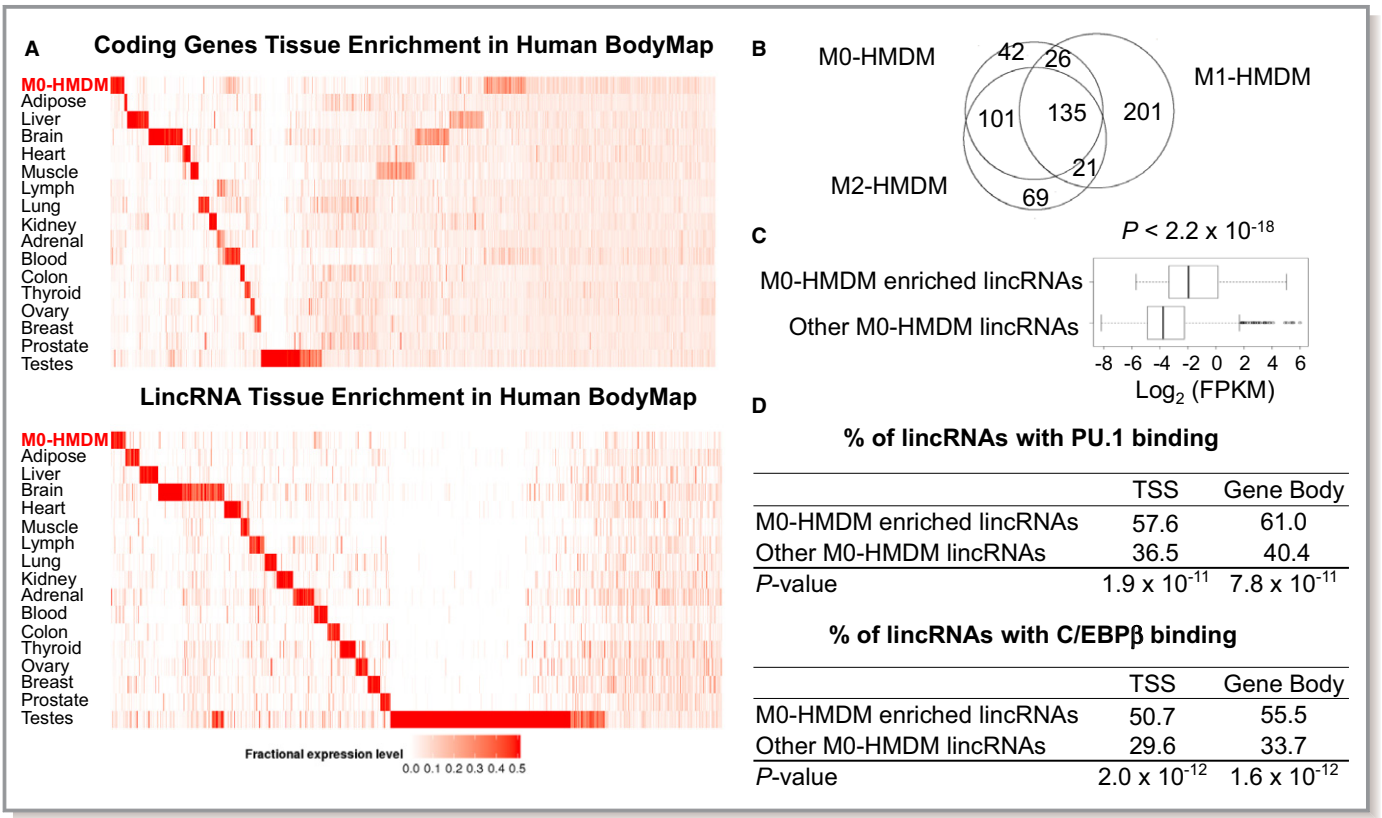

	TSS	Gene Body
M0-HMDM enriched lincRNAs	57.6	61.0
Other M0-HMDM lincRNAs	36.5	40.4
P-value	1.9×10^{-11}	7.8×10^{-11}

	TSS	Gene Body
M0-HMDM enriched lincRNAs	50.7	55.5
Other M0-HMDM lincRNAs	29.6	33.7
P-value	2.0×10^{-12}	1.6×10^{-12}

Figure 3. Tissue enrichment of macrophage lincRNAs. A, Relative abundance of mRNA and lincRNA genes (rows) expressed in M0 HMDM across 16 human tissue types from the Human BodyMap demonstrate that macrophage lincRNAs were more tissue-specific than mRNAs. Color intensity represents the fractional gene-level expression across all tissues examined, as described.[25] B, Certain lincRNAs were specifically enriched only in M1 or M2 HMDM. C, Expression of M0 HMDM-enriched lincRNAs were higher than that of nonenriched lincRNAs. D, Most M0 HMDM-enriched lincRNAs harbor PU.1 and C/EBPβ binding sites in ±2-kb intervals centered on the lincRNA TSS and gene body, and this percentage was higher than that in nonenriched M0 HMDM lincRNAs. HMDM indicates human peripheral blood mononuclear cell–derived macrophages; lincRNA, long intergenic noncoding RNA; TSS, transcription start site.

C/EBPβ binding sites, and most (72 of 114) were also macrophage enriched (Figure S4C and S4D). This highlights the potential roles of a subset of highly macrophage-specific lincRNAs in macrophage maturation and function.

Regulatory Features of Macrophage lincRNAs

Regulatory features at lincRNA loci increase the likelihood of biological and functional roles. Many macrophage lincRNAs overlap macrophage enhancer marks. Using public human macrophage chromatin immunoprecipitation sequencing data sets,[21] the majority of protein-coding genes (15 201 genes) displayed punctate binding of the H3K4me3 promoter mark around the TSS (±1.5 kb). In contrast, lincRNA TSS intervals showed relatively weaker signals, and only a small subset displayed high H3K4me3 density. In contrast, binding of H3K4me1, an enhancer mark, at lincRNAs was greater than at protein-coding genes (Figure 4A). Transcription from putative enhancer regions characterized by high levels of H3K4me1 relative to the H3K4me3 is a major feature of enhancer RNAs,[38] and lncRNAs that act as enhancer RNAs have been shown to modulate monocyte immune response.[39] For macrophage lincRNAs, we used H3K4me1/H3K4me3 ratios of >1.2 and <0.8 to define enhancer and promoter states,[39] respectively. In contrast to the predominance of promoter features at mRNAs (Figure 4A and Table S5), the majority of macrophage lincRNAs

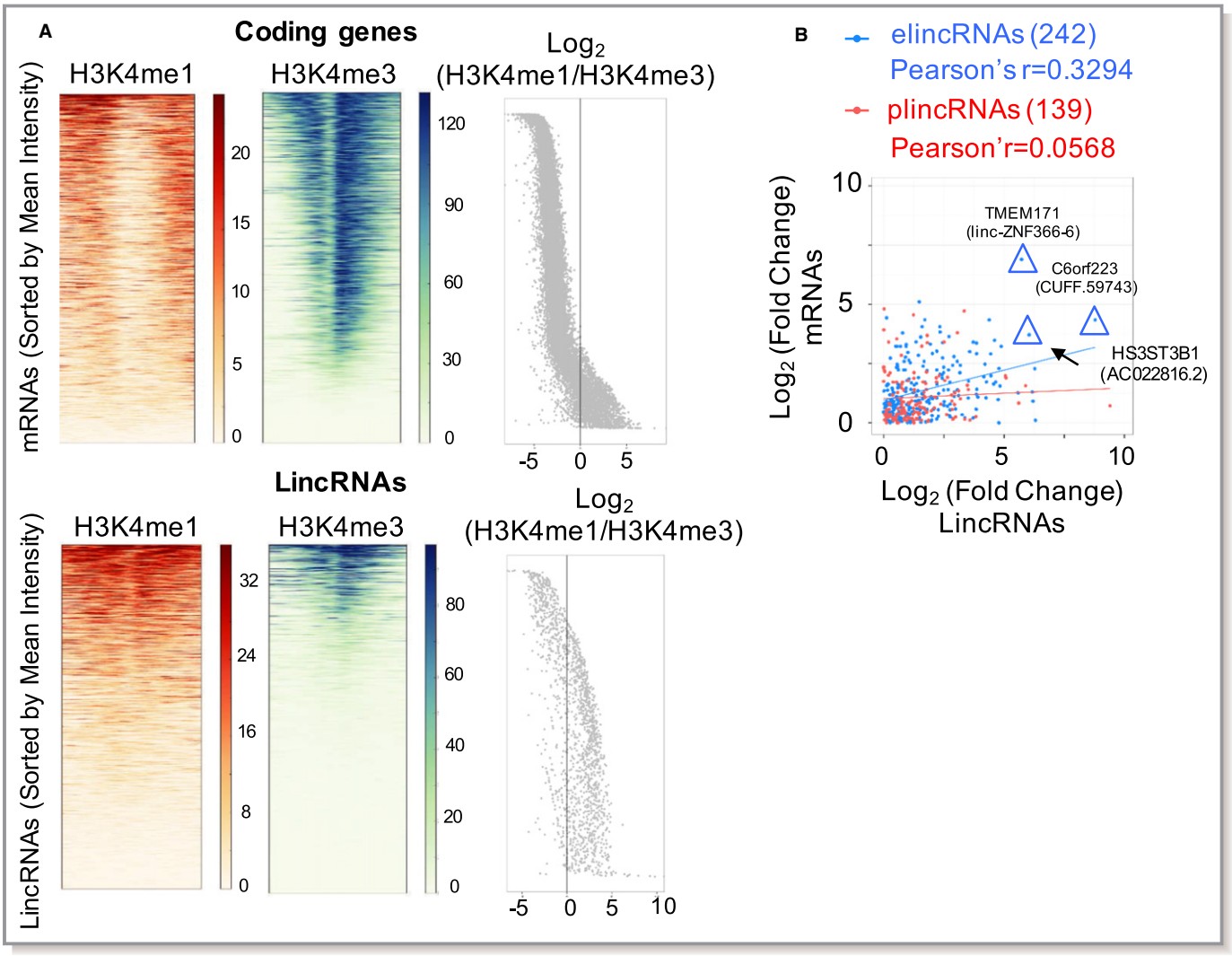

Figure 4. Macrophage lincRNAs have distinct enhancer-driven transcript signatures. A, Histone modification of H3K4me3 (promoter mark) and H3K4me1 (enhancer mark) across the ±1.5-kb region around the transcription start site and the H3K4me1/H3K4me3 ratios of protein-coding genes and lincRNAs show distinct enhancer-driven transcript signatures in macrophage lincRNAs vs protein-coding genes. Profiles were sorted based on mean H3K4me3 intensity. B, We used H3K4me1/H3K4me3 ratios of >1.2 and <0.8 to define enhancer and promoter states,[39] respectively. The correlation of fold change in expression during M1 activation (M0 vs M1) of "elincRNAs" and their closest protein-coding genes was significantly stronger than that for "plincRNAs." elincRNA indicates enhancer-associated lincRNA; H3K4me1, histone H3 lysine 4 monomethylation; H3K4me3, histone H3 lysine 4 trimethylation; lincRNA, long intergenic noncoding RNA; plincRNA, promoter-associated lincRNA.

(60.9%, 994 of a total of 1632 M0-HMDM lincRNAs with H3K4me1 and H3K4me3 signals) exhibited an H3K4me1/H3K4me3 ratio of >1.2, suggestive of "elincRNAs" with potential enhancer functions based on bioinformatics prediction (Table S5). Furthermore, elincRNAs were more macrophage enriched but had lower expression levels compared with promoter-associated lincRNAs, or "plincRNAs." Consistent with previous findings in mouse erythroblasts,[40] the polyadenylated macrophage elincRNAs in our catalog were more likely to have unidirectional transcription (Figure S5A through S5C), unlike most nonpolyadenylated bidirectional enhancer RNAs.[38]

We hypothesized that elincRNAs that overlap enhancer signatures (H3K4me1/H3K4me3 >1.2), would have greater coregulation with nearby protein-coding genes during M1 activation than lincRNAs with classical promoter signatures (H3K4me1/H3K4me3 <0.8). The correlation of fold change in expression during M1 activation (M0 versus M1) of elincRNAs and their closest protein coding genes was significantly stronger than that for plincRNAs (Z test, P=0.0039; Figure 4B). Gene ontology analysis of the 194 protein-coding genes nearest the M1-induced elincRNAs revealed enrichment for mRNAs involved in immune response and response to bacteria as well as transcriptional regulation (Figure S5D and Table S7). Ingenuity pathway analysis also suggested M1 activation related signaling and biological functions (Figure S5E and S5F and Tables S8 and S9). Indeed, a number of elincRNAs were paired with neighboring protein-coding genes known to have roles in the macrophage inflammatory response, including Acyl-CoA Synthetase Long-Chain Family Member 1 (proximal to RP11-701P16.5), Interleukin 6 (proximal to AC002480.2), C-C Motif Chemokine Ligand 8 (proximal to CUFF.135177), Interferon Induced Transmembrane Protein 3 (proximal to RP11-326C3.12), and Heparan Sulfate-Glucosamine 3-Sulfotransferase 3B1 (proximal to AC022816.2), or novel GWAS genes, such as Transmembrane Protein 171 (proximal to linc-ZNF366-6) associated with serum urate and gout,[41] and Chromosome 6 Open Reading Frame 223 (proximal to CUFF.59743 and CUFF.59265), associated with circulating levels of vascular endothelial growth factor[42] (see Table S10 for complete list). The genomic structure and the potential *cis*-regulatory effects of these elincRNAs on their coding gene partners require further functional investigation.

Thus, macrophage enrichment and TF binding patterns facilitate prioritization of macrophage lincRNAs that are more likely to be functional, whereas enhancer features suggest mechanistic avenues to pursue in translation.

M1 Activation Induced Widespread Changes in lincRNA Expression

Macrophage activation induces widespread change in the protein-coding gene transcriptome,[18] but lincRNA modulation during macrophage activation is largely unexplored. During M1 activation, 96 lincRNAs were DE (fold change >2, FDR-adjusted P<0.01), with 73 up- and 23 downregulated, of which 22 were newly annotated (Figure 5A and Table S11). In contrast to M1 activation, only 5 lincRNAs were DE (all upregulated) during M2 activation (Figure 5B; Table S12), consistent with the modest difference in mRNAs between IL-4–derived M2 HMDM and their macrophage colony-stimulating factor–differentiated M0 HMDM.[18] Relative to all macrophage lincRNAs, those that were DE during macrophage activation were more likely to be syntenic and annotated as expressed in mouse (15% versus 27%; P=0.0013), suggesting that synteny may be a feature of some physiologically relevant macrophage lincRNAs. In contrast, primary sequence conservation with mouse was not associated with DE lincRNAs in macrophage activation (≈25% in both groups). We focused further on lincRNAs that were upregulated in M1 or M2 activation and also macrophage-enriched, because mRNAs with such features have been shown to contain many important protein-coding genes with functional roles in macrophage biology.[18,43] Indeed, relative to noninduced lincRNAs, activation-induced lincRNAs (73 M1-induced and 5 M2-induced DE lincRNAs) were more likely to be macrophage-enriched (55 of 78, $P<2.2\times10^{-16}$) and to overlap PU.1 and C/EBPβ binding ($P=3.94\times10^{-3}$ and $P=3.39\times10^{-3}$, respectively, in TSS and $P=9.04\times10^{-5}$ and $P=2.96\times10^{-5}$, respectively, in gene body). These data highlight a promising subset of human macrophage lincRNAs for follow-up.

Based on abundance, extent of induction, tissue enrichment, and TF binding, we selected 10 lincRNAs (8 most upregulated in M1 activation and 2 most upregulated in M2 activation) for qRT-PCR validation and translational exploration. Using a set of independent macrophage samples (n=8 subjects), qRT-PCR analysis replicated the pattern of activation-induced lincRNA expression identified at RNA-seq for all lincRNAs (Figure 5C for M1-induced, and Figure 5D for M2-induced). Of these, MIR155HG is nonsyntenic; RP11-10J5.1, RP11-701P16.5, CTB-41I6.2, and RP5-836N10.1 are syntenic but not annotated as expressed in mouse; and linc-HEATR6-2, linc-SLC39A10-10, MIR146A, RP4-794H19.4 and RP11-184M15.1 are syntenic and annotated in mouse (Figure 5C and 5D). None of these lincRNAs showed significant sequence conservation in mouse. Of these 10 lincRNAs, 6 had enhancer-like histone signatures (see Table S13 for a summary). As an example, we showed the qRT-PCR validation of CUFF.15750, one of the most abundantly expressed de novo annotated lincRNAs, which was suppressed during both M1 and M2 activation and has PU.1 and C/EBPβ binding and enhancer-like features. Public cap analysis of gene expression peak data were consistent with the apparent TSS for CUFF.15750 revealed by our RNA-seq (Figure S6).

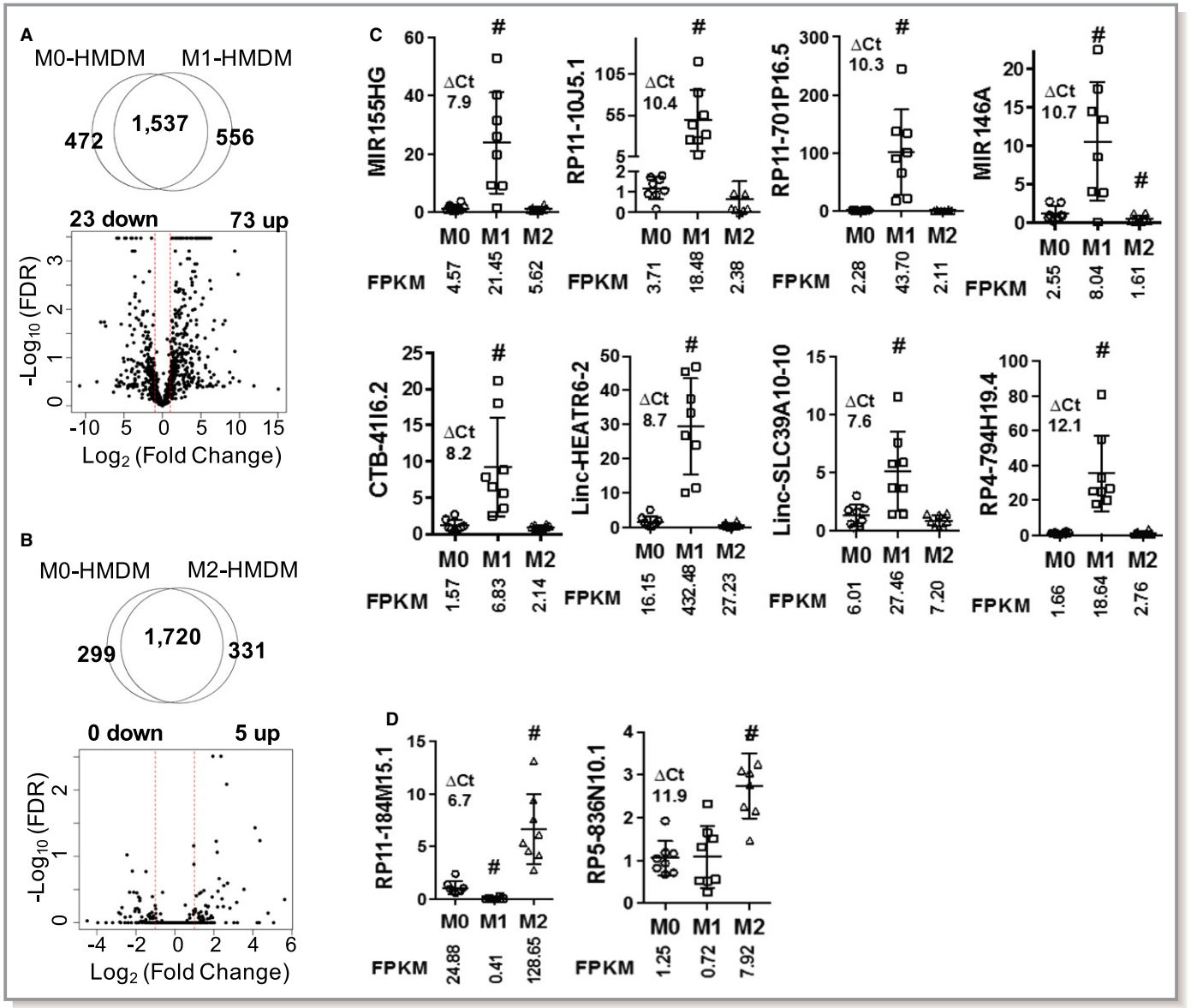

Figure 5. Macrophage activation induced widespread changes in lincRNA profile. Venn diagrams and volcano plot tabulating numbers of lincRNAs common or differentially expressed (fold change >2, FDR-adjusted $P<0.01$) between M0 HMDM vs M1 HMDM (A) and M0 HMDM vs M2 HMDM (B). C and D, Ten lincRNAs were selected according to prioritization criteria described in text. The relative expression levels of these lincRNAs in M0, M1, and M2 HMDM were determined using qRT-PCR and presented graphically, and the respective FPKM levels determined by RNA sequencing were listed showing consistent patterns with qRT-PCR results. The ΔCt represents the mean cycle threshold for lincRNAs relative to human ACTB mRNA as the reference in each sample. Data were shown as mean±SD, $^{\#}P<0.05$ vs M0 HMDM. FDR indicates false discovery rate; FPKM, fragments per kilobase of transcript per million fragments mapped; lincRNA, long intergenic noncoding RNA; qRT-PCR, quantitative reverse transcriptase–polymerase chain reaction.

GWASs Reveal Potential Disease-Associated Macrophage lincRNAs

The majority of genetic variants associated with complex diseases are found within noncoding regions of the genome, where the functional consequences of the variation are largely unknown. Consequently, we explored the overlap of macrophage lincRNAs with disease-associated genetic variations in public data sets. First, to probe broadly whether macrophage lincRNAs may underlie disease associations, we explored genomic loci for the 595 macrophage-enriched lincRNAs that contained SNP data within the comprehensive GWAS catalog[27] with trait associations of $P<1\times10^{-5}$. We identified 66 macrophage-enriched lincRNAs containing trait-associated SNPs and highlighted those traits for which macrophages have been implicated, including metabolic (eg, obesity-related traits, visceral fat, and waist–hip ratio) and immune disorders (eg, Crohn disease, multiple sclerosis, and celiac disease; boldface in Table S14).

Second, because of the central role of macrophage activation in multiple CMDs, we interrogated SNPs within all macrophage-expressed lincRNAs for their specific association with 13 cardiometabolic traits (Table S2). Of the 2766 macrophage-expressed lincRNAs, 2340 lincRNAs contained SNPs that were tested in at least 1 of the 13 GWAS data sets. Using our published pipelines,[20,30] lincRNAs containing significant trait-associated SNPs were filtered stringently to include only those that contained the strongest and independent (r^2<0.3; based on 1000Genomes CEU data[44]) SNP-level *P* value in the region (±500 kb of the lincRNA; see Methods for details). By further filtering for the most prominently expressed lincRNAs (FPKM >0.1, corresponding to top ≈35% expressed macrophage lincRNAs), we identified 3 independent trait-associated SNPs—for waist-to-hip ratio adjusted for body mass index, plasma triglycerides, and plasma low-density lipoprotein-cholesterol—that fall within ±1 kb of highly expressed macrophage lincRNAs (Table).

A top trait association is at a lincRNA annotated as RP11-472N13.3, which we named MacORIS. MacORIS overlaps rs7081678, an SNP associated with central obesity (waist–hip ratio adjusted for body mass index); maps to the chromosome 10p11.22 locus (Figure 6A through 6C); and is a macrophage-enriched lincRNA that is syntenic but not annotated in mouse. MacORIS is expressed predominantly in M0 HMDM (fractional expression value: 0.44), is barely detectable in human primary adipocytes, and is found at low levels in human adipose cells (Figure 6D) and T cells (Figure 6E). A genome browser view of MacORIS shows abundant PU.1 and C/EBPβ binding (Figure 6F) but no annotation in Genome Reference Consortium Mouse Build 38 (GRC38/mm10) and no expression in published high-quality RNA-seq of murine bone marrow–derived macrophages (Figure 6G and Table S15). MacORIS does not contain a conserved open reading frame, and in vitro transcription and translation of MacORIS did not produce any detectable peptides (Figure S7A). The qRT-PCR of cell fractions revealed that MacORIS is predominantly located in cytoplasm (Figure 6H), suggesting potential posttranscriptional regulatory roles. M1, but not M2, stimulation suppressed MacORIS expression (Figure 6I and 6J). To examine the functional impact of MacORIS on M1 activation, we used GapmeR antisense oligonucleotide to knock down MacORIS in THP-1Φ and found enhanced expression of IFN-γ–induced negative regulators *SOCS1* and *SOCS3* but no effect on lipopolysaccharide-induced inflammatory genes such as *TNF*, *TNFAIP3*, and *IL1B* (Figure 6K). Cytoplasmic localization suggests that MacORIS modulates cytoplasmic activation, rather than nuclear expression, of IFN-γ–signaling molecules. IFN-γ activates IFNGR1 and IFNGR2, via transphosphorylation of JAK1 and JAK2 and with downstream phosphorylation of STAT1 leading to oxidative burst and expression of IFN-γ–inducible genes, including *IL12*.[45] Knockdown of MacORIS in THP-1Φ enhanced the phosphorylation of STAT1 without altering total protein levels of IFNGR1, JAK2, or STAT1 (Figure 6L and 6M). Independent validation in M1 THP-1Φ with knockdown of MacORIS by small interfering RNA showed generally consistent results except that knockdown of MacORIS enhanced JAK2 as well as STAT1 phosphorylation (Figure S7B and S7C); this difference may be attributable to the differential activity and mechanisms of antisense oligonucleotide– versus small interfering RNA–mediated knockdown for nuclear relative to cytoplasmic targets. Overall, these data suggest that cytoplasmic MacORIS serves as a repressor of macrophage IFN-γ signal transduction by modulating, via as-yet-unknown mechanisms, JAK2/STAT1 phosphorylation, thus regulating downstream IFN-γ–responsive gene expression. Whether the central obesity–associated SNPs at this locus modulate MacORIS expression and function remains to be

Table. Cardiometabolic Trait-Associated Genetic Variants at Macrophage lincRNAs

LincRNA	Position	Exons	Traits	Nearby Candidate Genes	Top SNP	Minimum *P* Value	Bonferroni-Adjusted *P* Value
MacORIS (RP11-472N13.3)	10:31982012-31996316	2	WHRadjBMI	…	rs7081678 *†	5.76E-07	3.50E-02
AP006216.11	11:116645826-116646592	2	Triglyceride	*BUD13,ZNF259,APOA5, SIK3,TAGLN,PCSK7*	rs11602073‡§	1.26E-10	7.90E-06
	11:116645826-116646592	2	LDL-C	*BUD13,ZNF259,APOA5, SIK3,TAGLN,PCSK7*	rs11602073‡§	4.00E-09	2.51E-04
Linc-BCL3	19:45240862-45250906	3	LDL-C	*APOE, APOC1*	rs1531517‡§	4.22E-99	2.64E-94

LDL-C indicates low-density lipoprotein cholesterol; lincRNA, long intergenic noncoding RNA; SNP, single nucleotide polymorphism; WHRadjBMI, waist–hip ratio adjusted for body mass index.

*SNP is in the lincRNA.

†SNP is the strongest signal in region.

‡SNP is not in the lincRNA.

§SNP is not the strongest signal but is in low-linkage disequilibrium (r<0.3) with the strongest signal.

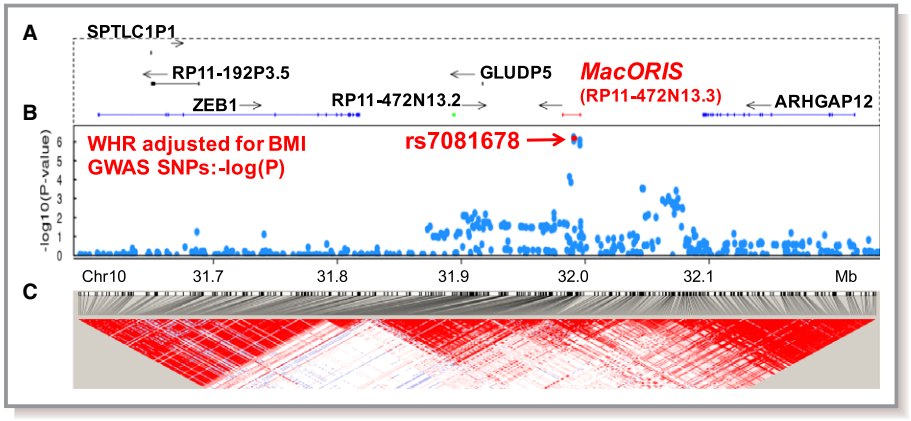

Figure 6. MacORIS harbors variant associated with central obesity and acts as a repressor of IFN-γ signaling. Genome browser view of MacORIS (annotated as RP11-472N13.3) locus on chr10 (A and B) and linkage disequilibrium plot in European ancestry (C) shows that MacORIS overlaps SNP rs7081678, which is associated with WHR adjusted for BMI. MacORIS is abundant in M0 HMDM and monocytes but found at low levels in human adipose tissue and stromal vascular fraction–differentiated adipocytes (D, by RNA-seq) and T cells (E, by qRT-PCR). (F) Genome browser view of RNA-seq tracks demonstrates lower expression level of MacORIS in M1 HMDM vs M0 HMDM, a consistent pattern also seen in M1 IPSDM vs M0 IPSDM. MacORIS has abundant PU.1 and C/EBPβ binding, both at transcription start site and gene body, in HMDM (F), but there was no annotation in mouse GRC38/mm10 and no expression in published RNA-seq of murine bone marrow–derived macrophages (G). H, MacORIS is located primarily in cytoplasm (I), and qRT-PCR validation confirmed that the expression of MacORIS was suppressed in M1 HMDM (n=8 subjects) and M1 THP1Φ (n=3 experiments). Because MacORIS was suppressed 6 h after M1 stimulation (J), the effects of knockdown of MacORIS were examined at 1 h after M1 stimulation. K, ASO induced 90% knockdown of MacORIS in M1 THP-1Φ. Knockdown of MacORIS enhanced the expression of IFN-γ–inducible genes, such as *SOCS1, SOCS3*, and *IL12*, but did not affect LPS-induced early response genes, such as *TNF, TNFAIP3*, and *IL1B*. L, Knockdown of MacORIS by ASO did not affect the cell surface protein expression of IFNGR1 but enhanced phosphorylation of components of IFN-γ downstream signaling pathways, including STAT1 (M), suggesting its role as a repressor of the IFN-γ signaling. n=3 separate experiments with triplicates. Data were mean±SEM. $^{\#}P<0.05$ by t test. ASO indicates antisense oligonucleotide; BMI, body mass index; CAGE, cap analysis of gene expression; CHiP-seq, chromatin immunoprecipitation sequencing; FACS, fluorescence-activated cell sorting; FPKM, fragments per kilobase of transcript per million fragments mapped; GWAS, genomewide association study; H3K4me1, histone H3 lysine 4 monomethylation; H3K4me3, histone H3 lysine 4 trimethylation; HMDM, human peripheral blood mononuclear cell–derived macrophages; IFN-γ, interferon γ; IFNGR1, IFN-γ receptor 1; IPSDM, induced pluripotent stem cell–derived macrophages; JAK2, Janus kinase 2; LPS, lipopolysaccharide; MacORIS, macrophage-enriched obesity-associated lincRNA serving as a repressor of IFN-γ signaling; MFI, mean fluorescence intensity; PBMC, peripheral blood mononuclear cells; qRT-PCR, quantitative reverse transcriptase–polymerase chain reaction; RNA-seq, RNA sequencing; SNP, single nucleotide polymorphism; STAT1, signal transducer and activator of transcription 1; THP-1Φ, THP-1 monocyte-derived macrophages; WHR, waist–hip ratio.

determined, but macrophage IFN-γ signaling by MacORIS is a very plausible mechanism for modulation of central obesity and related metabolic disorders at this locus.[46]

LincRNAs Are Expressed and Modulated Similarly in Human IPSDMs and Primary HMDMs

It is important to consider human-relevant strategies and to develop tools for functional interrogation of human lincRNAs not expressed in mouse. IPSDMs are a renewable source of subject-specific macrophages and provide a powerful functional genomic tool to address human macrophage biology. We reported previously that IPSDMs had comparable phenotypes, protein-coding transcriptomes, and functional characteristics as HMDMs and can be used for functional genomic modeling of protein-coding genes.[18] In this article, we extended our IPSDM model for our current lincRNA perspective by examining DE lincRNAs between induced pluripotent

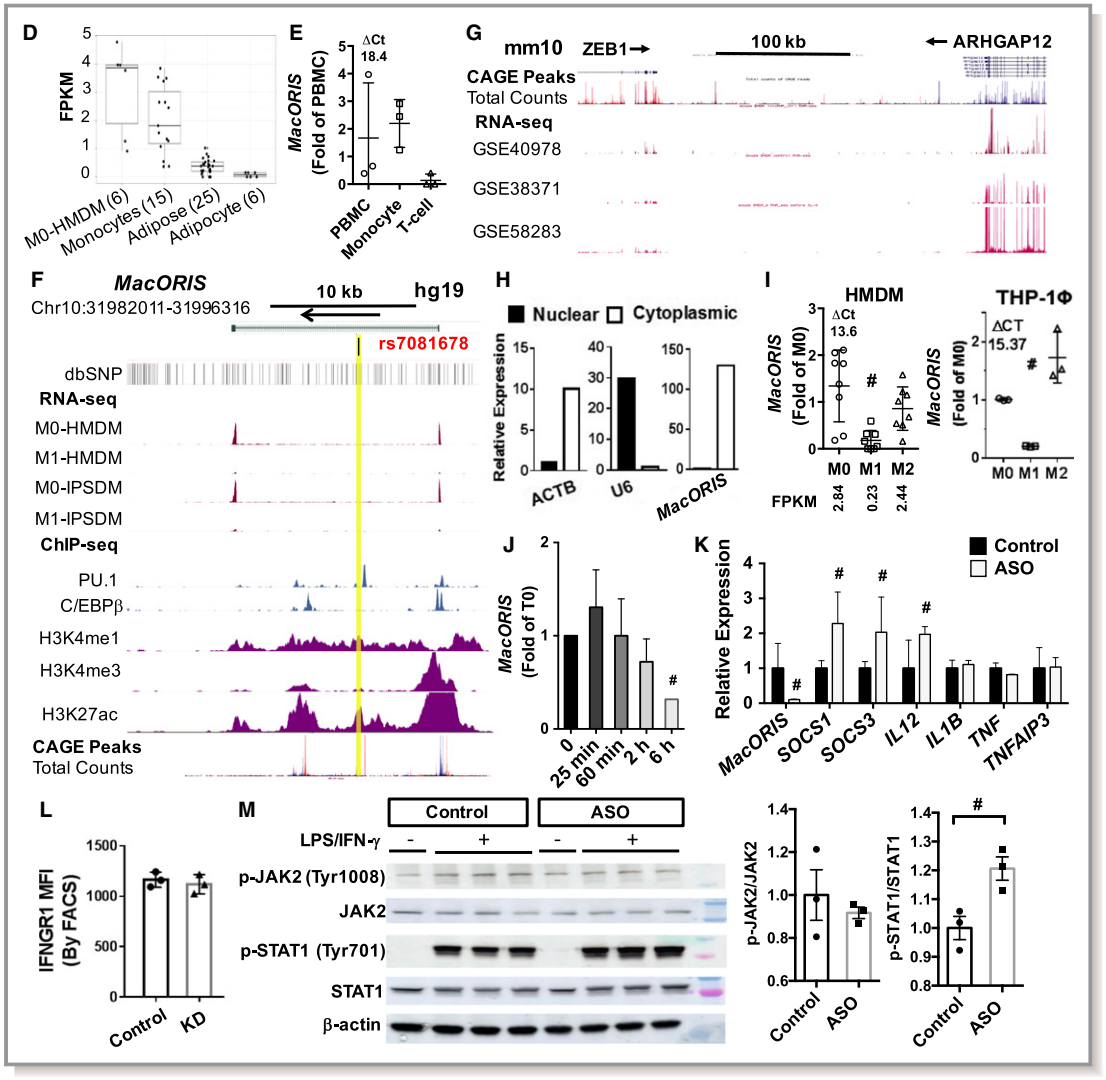

Figure 6. Continued.

stem cells and IPSDMs and comparing resting and activation profiles of lincRNAs in IPSDMs versus HMDMs (Figure 7A).[18] A multidimensional scaling plot based on expression of lincRNAs (Figure 7B) revealed that HMDMs and IPSDMs cluster together and are completely distinct from induced pluripotent stem cells; M1 HMDMs and M1 IPSDMs also cluster together and separately from M0 or M2 HMDMs. Differentiation of induced pluripotent stem cells to IPSDMs induced marked lincRNA transcriptome changes with 313 DE lincRNAs. Compared with all other IPSDM lincRNAs, the 153 lincRNAs upregulated during differentiation of induced pluripotent stem cells to IPSDMs (Figure 7C and Table S16) had higher expression (Figure 7D) and had enriched PU.1 and C/EBPβ TF binding (Figure 7E).

The vast majority (>90%) of the M0 HMDM lincRNAs were also present in M0 IPSDMs, and their expression was moderately correlated (r=0.51; Figure 7F). Remarkably, for ≈95% of lincRNAs, there was a similar pattern of activation-related change in expression in both HMDMs and IPSDMs with strong correlations (eg, r=0.81 between IPSDMs and HMDMs for M1-activation–induced fold change of lincRNAs; Figure 7G and 7H; Tables S11 and S12). Indeed, only very few lincRNAs were DE between HMDMs and IPSDMs (Figure 7F and Table S17). For the very small number of lincRNAs that were expressed at lower levels in M0 IPSDMs than in M0 HMDMs (eg, linc-SLC39A10-10), on activation, their expression in M1 or M2 IPSDMs was comparable to that in M1 or M2 HMDMs (Table S18). As a relevant example, a genome browser view of MacORIS shows consistent expression patterns for HMDMs and IPSDMs at rest and during M1 activation (Figure 6F). Overall, IPSDM lincRNA expression and activation profiles resemble those of HMDMs, supporting the utility of the IPSDM system for functional modeling of lincRNAs in human macrophage genomics.

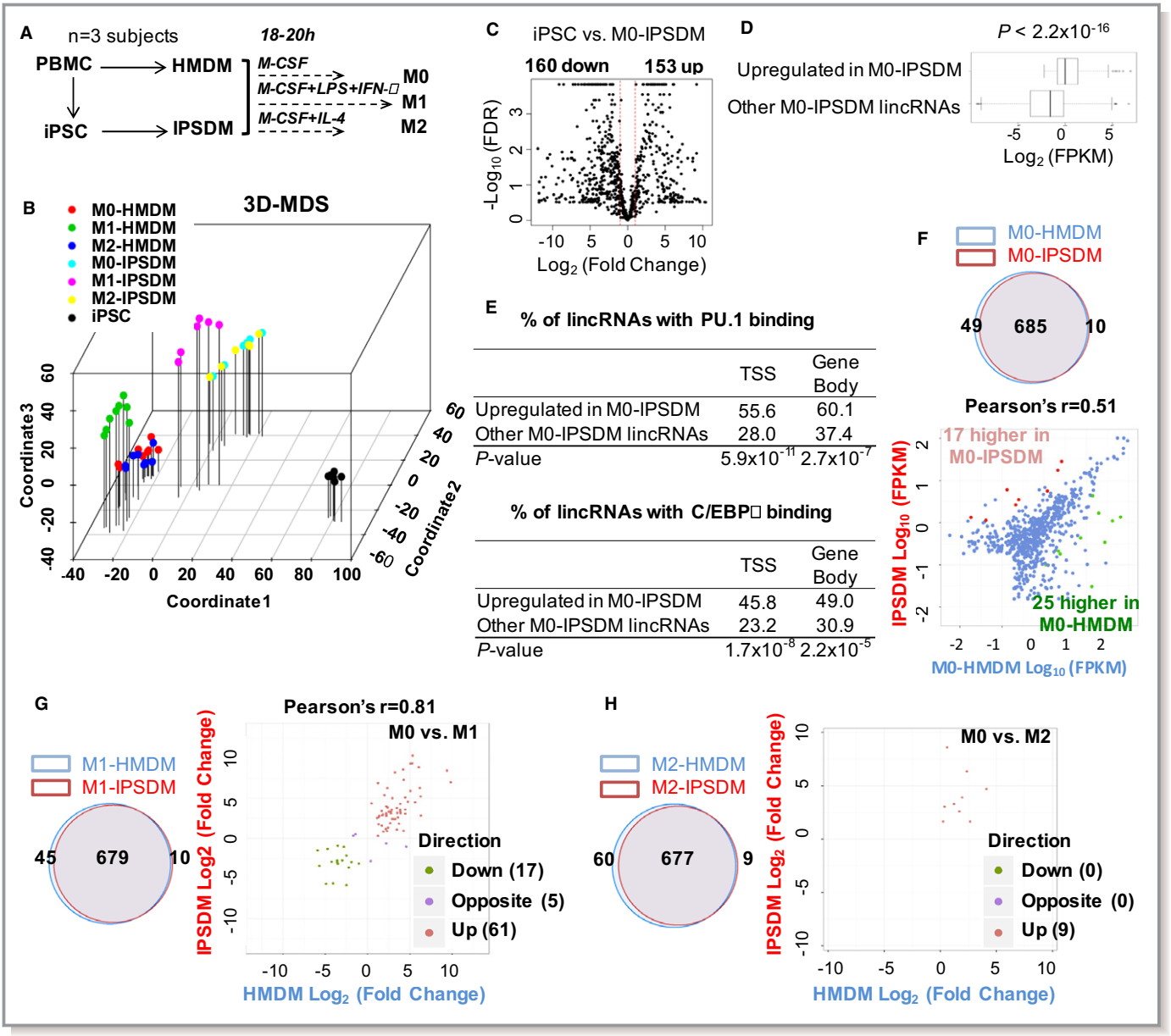

Figure 7. IPSDM resembles the lincRNA expression and activation profiles of HMDM. A, Schematic figure of HMDM and IPSDM differentiation and activation. B, Multidimensional scaling plot confirmed distinct lincRNA transcriptome profile of iPSC from HMDM and IPSDM. M1 activation profoundly influences the lincRNA expression profile, whereas M2 activation resulted in more subtle expression changes in both HMDM and IPSDM. C, iPSC-to-IPSDM differentiation induced profound lincRNA expression changes, with 160 higher in iPSC and 153 higher in IPSDM (n=3 subjects). D, LincRNAs upregulated during iPSC-to-IPSDM differentiation were more abundantly expressed and demonstrated enriched PU.1 and C/EBPβ binding (E). F, Venn diagram shows remarkable overlap of lincRNA expression between M0 HMDM and M0 IPSDM (n=3 subjects). A small number (n=42) of lincRNAs were differentially expressed between HMDM and IPSDM with 25 higher in M0 HMDM and 17 higher in M0 IPSDM. G and H, IPSDM resembled lincRNA profiles of HMDM for both M1 and M2 activation. FDR, false discovery rate; FPKM, fragments per kilobase of transcript per million fragments mapped; HMDM, human peripheral blood mononuclear cell–derived macrophages; IL-4, interleukin 4; INF-γ, interferon γ; iPSC, induced pluripotent stem cells; IPSDM, induced pluripotent stem cell–derived macrophages; lincRNA, long intergenic noncoding RNA; LPS, lipopolysaccharide; M-CSF, macrophage colony-stimulating factor; PBMC, peripheral blood mononuclear cells; 3D-MDS, 3-dimensional multidimensional scaling; TSS, transcription start site.

Discussion

Macrophages modulate many human pathophysiologies and have emerged as potential therapeutic targets in complex diseases.[5] Although a recent microarray-based study has characterized lncRNAs in M1- and M2-activated HMDMs,[14] there is a lack of RNA-seq–based, unbiased cataloging of the human macrophage lncRNA transcriptome. By exploiting de novo transcriptome reconstruction of deep RNA-seq data, we provide the most comprehensive inventory and genomic

profile, to our knowledge, of polyadenylated human macrophage lincRNAs. We identified 2766 macrophage-expressed lincRNAs, 861 of which are newly annotated. Most (85%) macrophage lincRNAs are nonsyntenic or are syntenic but not annotated as expressed in mouse. Many lincRNAs are enriched in macrophages, overlap PU.1 and C/EBPβ transcription factor binding sites, and display enhancer-like chromatin signatures, and multiple macrophage-enriched lincRNAs were also found to overlap GWAS loci for CMD traits. Macrophage activation, particularly to the M1 phenotype, markedly alters the lincRNA expression profiles, suggesting a role for lincRNAs in macrophage functional activation. MacORIS, a human macrophage-specific cytoplasmic lincRNA that contains SNPs associated with central obesity, functions as a brake on macrophage IFN-γ signaling and inflammatory responses. Finally, because many human macrophage lincRNAs are not conserved in mouse, our efficient and scalable human IPSDM system provides a valuable cellular model for functional assessment of lincRNAs in human macrophage biology.

Although reductionist relative to in vivo phenotype complexity, in vitro activation to M1 or M2 macrophage phenotypes has proven useful in defining functional states toward which macrophages can be driven in distinct inflammatory milieu.[6,7] For example, multiple macrophage protein-coding genes (eg, *IL6*, *TNF*, *IL1B*) of functional importance are markedly induced during M1 activation in vitro and in vivo.[18] Consistent with the pattern for mRNAs,[7–9,18] M1 activation induces profound changes in lincRNA expression with induction of dozens of lincRNAs. Correlation of activation-dependent change in enhancer lincRNA expression with that of the nearest protein-coding genes maps to regulation of immune system processes and suggests an integrative regulatory role for some lincRNAs during macrophage activation. Indeed, through our prioritization strategy, we identified that lincRNAs reported previously to modulate myeloid cell functions (eg, linc-HEATR6-2, also named lnc-DC) were recently reported to regulate dendritic cell maturation and function.[47] Furthermore, 2 prioritized lincRNAs, MIR155HG and MIR146A, are microRNA host genes for miR-155[48] and miR-146a,[49] 2 well-characterized microRNAs that regulate macrophage inflammatory responses.[48,49] This strategy identified multiple other lincRNAs as promising *cis*-regulatory candidates for functional and translational interrogation (eg, AC002480.2 proximal to IL6 and CUFF.135177 proximal to CCL8). A recent in vitro RNA-seq study of lipopolysaccharide-stimulated (4 hours) monocytes discovered DE lncRNAs that modulate monocyte response to lipopolysaccharide.[39] We identified 49 DE lincRNAs induced in lipopolysaccharide-treated monocytes, and 14 of these overlapped lincRNAs also upregulated during M1 HMDM activation. Nevertheless, a much larger proportion (59 of 73) of lincRNAs induced during M1 activation are not identified in monocyte activation, suggesting specific macrophage induction and function (Table S19). M1 and M2 activation in vitro, however, provides a relatively narrow window into the diversity of macrophage activation states observed in vivo; future transcriptional profiling of resident macrophages across diverse tissues and settings will provide deeper insight into the in vivo complexity of the human macrophage noncoding transcriptome.

Recent GWASs have revealed novel functional lncRNAs in disease, for example, ANRIL at the 9p21.3 locus for coronary heart disease[50] and Lnc13 at 2q12.1 for celiac disease.[51] These human genetic studies suggest that lincRNAs may play important modulatory roles in human diseases. Indeed, we identified hundreds of macrophage lincRNAs that reside within intergenic loci previously identified by GWASs for complex traits. We performed a deeper interrogation of lincRNAs in 13 CMD data sets and identified several promising candidates including MacORIS, which we found to act as a repressor of IFN-γ signaling by regulating phosphorylation of JAK2 and STAT1. Notably, IFN-γ deficiency protects mice from high fat diet–induced white adipose tissue inflammatory cell accumulation and glucose tolerance.[46] Thus, MacORIS modulation of IFN-γ signaling in macrophages is a plausible mechanism underlying the 10p11.22 locus for central obesity. However, the causal variant at MacORIS and the precise genetic and cellular mechanisms of action of MacORIS require further investigation.

MacORIS is one of many human lincRNAs not present in mice. This lack of conservation combined with historical limitations of human macrophage models presents a specific challenge to functional studies of lincRNAs in human macrophage biology. RNA interference and antisense oligonucleotide–based knockdown approaches in primary monocytes and macrophages are challenging, given low transfection rates and heterogeneity between experiments. THP-1 monocyte and macrophage lines, although useful, as we demonstrate for MacORIS, are karyotypically abnormal and phenotypically immature,[15] thus also not an ideal model for human functional genomics. We developed a high-fidelity model for human macrophage functional genomics studies.[18] Our results in this study reveal comparable lincRNA transcriptome profiles and dynamic regulation during activation in isogenic IPSDMs and HMDMs. Coupled to CRISPR/Cas9 gene editing that precisely introduces targeted mutations and deletions,[52] IPSDM provides a powerful tool to decipher the genomic and molecular regulation of human macrophage lincRNAs in human physiology and disease.

Recently, the FANTOM CAT (CAGE-associated transcriptome)—a human transcriptome meta-assembly based on cap analysis of gene expression data across 1829 samples from major human primary cell types and tissues as well as transcript models from GENCODE V19, the Cabili set,

miTranscriptome, and ENCODE—has defined 27 919 lncRNAs, of which 13 105 were lincRNAs.[53] We found 901 of 2766 of our macrophage lincRNAs overlapped FANTOM CAT lincRNAs within ±250 bp of the TSS (Table S20). Because the FANTOM5 CAT included human macrophages from only 3 donors, additional macrophage lincRNAs will be added to such public resources as sample size and sequencing depth increase, as in our study. Nonetheless, the precise 5′-end transcript mapping in FANTOM5 CAT lincRNAs is complementary to but less comprehensive than our deep RNA-seq–based human macrophage lincRNA catalog.

In the current work, we focused on lincRNAs for both technical and translational reasons. LncRNAs that either overlap (ie, antisense) or share a TSS interval with protein-coding genes confound simple interpretation of regulatory features in the region and complicate genetic manipulation in functional studies. There are also analytic challenges in dissecting the contribution of GWAS disease-associated SNPs residing in lncRNAs that overlap protein-coding genes. Consequently, lncRNAs excluded from our analysis, including lincRNAs proximal to the coding genes, antisense lncRNAs shown to regulate THP-1Φ function,[54] and single-exon transcripts are likely to provide additional layers of information about the macrophage noncoding transcriptome.

Our study has many strengths but limitations too. Our lincRNA catalog derived from poly(A) capture RNA-seq fails to include nonpolyadenylated lncRNAs and short noncoding RNAs. It has been reported that 84.2% and 74.2% of the annotated expressed lncRNAs are poly(A)+ in H9 and Hela cells, respectively; 13.1% and 23.3% are bimorphic, found in both the poly(A)+ and poly(A)− populations, respectively; and 2.7% and 2.5% are poly(A)−, suggesting the majority of the lncRNAs are poly(A)+ or bimorphic, respectively.[55] The classification, however, has not been performed in human macrophage. Coding potential was assessed by computational prediction using iSeeRNA[33] and Pfam[34] with validation by PhyloCSF[35] but not with experimental approaches. A fully comprehensive macrophage lncRNA catalog derived from RNA-seq of ribosomal RNA–depleted samples combined with both bioinformatic and experimental approaches for coding potential assessment will further refine the human macrophage lncRNA catalog for future study. In the meantime, a large number of prioritized lincRNAs in our study remains to be functionally validated to gain deeper mechanistic insights into lincRNA modulation of human macrophage biology and their role in human diseases.

Our work underscores the importance of lincRNA discovery studies, using deep RNA-seq and de novo assembly, in a species- and tissue-specific manner. It also provides a resource to parse the polyadenylated lincRNA circuitry of macrophage activation and to identify specific lincRNAs for functional studies in macrophage activation and macrophage-related human diseases, as we have explored for MacORIS. Our IPSDM model provides a unique framework with which to pursue the human macrophage–specific functions of novel lincRNAs in macrophage biology and related diseases and for gene-editing strategies to advance mechanism-based clinical and therapeutic translation of human genomic discoveries.

Sources of Funding

This work was supported by National Institutes of Health (NIH) grants R01-HL-113147 (to Reilly and Li), R01-HL-132561 (to Reilly), K24-HL-107643 (to Reilly), and U01-HG006398 (to Rader and Morrisey). Reilly is also supported by NIH R01-HL-111694. Li is also supported by NIH R01-GM-108600. H. Zhang is supported by NIH K99-HL-130574. Yang and the University of Pennsylvania Induced Pluripotent Stem Cell Core Facility are supported by the University of Pennsylvania Institute for Regenerative Medicine. Research reported in this publication also used the resources of Columbia University's Cancer Center Flow Core Facility funded in part through NIH Center Grant P30CA013696, and Columbia's CCTI Flow Cytometry Core, supported in part by the Office of the Director, NIH under awards S10RR027050. The content is solely the responsibility of the authors and does not necessarily represent the official views of the NIH.

Disclosures

None.

References

1. Ulitsky I, Bartel DP. Lincrnas: genomics, evolution, and mechanisms. *Cell*. 2013;154:26–46.
2. Uchida S, Dimmeler S. Long noncoding RNAs in cardiovascular diseases. *Circ Res*. 2015;116:737–750.
3. Cabili MN, Trapnell C, Goff L, Koziol M, Tazon-Vega B, Regev A, Rinn JL. Integrative annotation of human large intergenic noncoding RNAs reveals global properties and specific subclasses. *Genes Dev*. 2011;25:1915–1927.
4. Zeller I, Srivastava S. Macrophage functions in atherosclerosis. *Circ Res*. 2014;115:e83–e85.
5. Wynn TA, Chawla A, Pollard JW. Macrophage biology in development, homeostasis and disease. *Nature*. 2013;496:445–455.
6. Huang SC, Everts B, Ivanova Y, O'Sullivan D, Nascimento M, Smith AM, Beatty W, Love-Gregory L, Lam WY, O'Neill CM, Yan C, Du H, Abumrad NA, Urban JF Jr, Artyomov MN, Pearce EL, Pearce EJ. Cell-intrinsic lysosomal lipolysis is essential for alternative activation of macrophages. *Nat Immunol*. 2014;15:846–855.
7. Beyer M, Mallmann MR, Xue J, Staratschek-Jox A, Vorholt D, Krebs W, Sommer D, Sander J, Mertens C, Nino-Castro A, Schmidt SV, Schultze JL. High-resolution transcriptome of human macrophages. *PLoS One*. 2012;7:e45466.
8. Martinez FO, Gordon S, Locati M, Mantovani A. Transcriptional profiling of the human monocyte-to-macrophage differentiation and polarization: new molecules and patterns of gene expression. *J Immunol*. 2006;177:7303–7311.
9. Xue J, Schmidt SV, Sander J, Draffehn A, Krebs W, Quester I, De Nardo D, Gohel TD, Emde M, Schmidleithner L, Ganesan H, Nino-Castro A, Mallmann MR, Labzin L, Theis H, Kraut M, Beyer M, Latz E, Freeman TC, Ulas T, Schultze JL. Transcriptome-based network analysis reveals a spectrum model of human macrophage activation. *Immunity*. 2014;40:274–288.
10. Carpenter S, Aiello D, Atianand MK, Ricci EP, Gandhi P, Hall LL, Byron M, Monks B, Henry-Bezy M, Lawrence JB, O'Neill LA, Moore MJ, Caffrey DR,

Fitzgerald KA. A long noncoding RNA mediates both activation and repression of immune response genes. *Science*. 2013;341:789–792.

11. Atianand MK, Hu W, Satpathy AT, Shen Y, Ricci EP, Alvarez-Dominguez JR, Bhatta A, Schattgen SA, McGowan JD, Blin J, Braun JE, Gandhi P, Moore MJ, Chang HY, Lodish HF, Caffrey DR, Fitzgerald KA. A long noncoding RNA lincRNA-EPS acts as a transcriptional brake to restrain inflammation. *Cell*. 2016;165:1672–1685.
12. Hu YW, Zhao JY, Li SF, Huang JL, Qiu YR, Ma X, Wu SG, Chen ZP, Hu YR, Yang JY, Wang YC, Gao JJ, Sha YH, Zheng L, Wang Q. RP5-833A20.1/miR-382-5p/NFIA-dependent signal transduction pathway contributes to the regulation of cholesterol homeostasis and inflammatory reaction. *Arterioscler Thromb Vasc Biol*. 2015;35:87–101.
13. Pawar K, Hanisch C, Palma Vera SE, Einspanier R, Sharbati S. Down regulated lncRNA MEG3 eliminates mycobacteria in macrophages via autophagy. *Sci Rep*. 2016;6:19416.
14. Huang Z, Luo Q, Yao F, Qing C, Ye J, Deng Y, Li J. Identification of differentially expressed long non-coding RNAs in polarized macrophages. *Sci Rep*. 2016;6:19705.
15. Daigneault M, Preston JA, Marriott HM, Whyte MK, Dockrell DH. The identification of markers of macrophage differentiation in PMA-stimulated THP-1 cells and monocyte-derived macrophages. *PLoS One*. 2010;5:e8668.
16. Consortium F, the RP, Clst, Forrest AR, Kawaji H, Rehli M, Baillie JK, de Hoon MJ, Haberle V, Lassmann T, Kulakovskiy IV, Lizio M, Itoh M, Andersson R, Mungall CJ, Meehan TF, Schmeier S, Bertin N, Jorgensen M, Dimont E, Arner E, Schmidl C, Schaefer U, Medvedeva YA, Plessy C, Vitezic M, Severin J, Semple C, Ishizu Y, Young RS, Francescatto M, Alam I, Albanese D, Altschuler GM, Arakawa T, Archer JA, Arner P, Babina M, Rennie S, Balwierz PJ, Beckhouse AG, Pradhan-Bhatt S, Blake JA, Blumenthal A, Bodega B, Bonetti A, Briggs J, Brombacher F, Burroughs AM, Califano A, Cannistraci CV, Carbajo D, Chen Y, Chierici M, Ciani Y, Clevers HC, Dalla E, Davis CA, Detmar M, Diehl AD, Dohi T, Drablos F, Edge AS, Edinger M, Ekwall K, Endoh M, Enomoto H, Fagiolini M, Fairbairn L, Fang H, Farach-Carson MC, Faulkner GJ, Favorov AV, Fisher ME, Frith MC, Fujita R, Fukuda S, Furlanello C, Furino M, Furusawa J, Geijtenbeek TB, Gibson AP, Gingeras T, Goldowitz D, Gough J, Guhl S, Guler R, Gustincich S, Ha TJ, Hamaguchi M, Hara M, Harbers M, Harshbarger J, Hasegawa A, Hasegawa Y, Hashimoto T, Herlyn M, Hitchens KJ, Ho Sui SJ, Hofmann OM, Hoof I, Hori F, Huminiecki L, Iida K, Ikawa T, Jankovic BR, Jia H, Joshi A, Jurman G, Kaczkowski B, Kai C, Kaida K, Kaiho A, Kajiyama K, Kanamori-Katayama M, Kasianov AS, Kasukawa T, Katayama S, Kato S, Kawaguchi S, Kawamoto H, Kawamura YI, Kawashima T, Kempfle JS, Kenna TJ, Kere J, Khachigian LM, Kitamura T, Klinken SP, Knox AJ, Kojima M, Kojima S, Kondo N, Koseki H, Koyasu S, Krampitz S, Kubosaki A, Kwon AT, Laros JF, Lee W, Lennartsson A, Li K, Lilje B, Lipovich L, Mackay-Sim A, Manabe R, Mar JC, Marchand B, Mathelier A, Mejhert N, Meynert A, Mizuno Y, de Lima Morais DA, Morikawa H, Morimoto M, Moro K, Motakis E, Motohashi H, Mummery CL, Murata M, Nagao-Sato S, Nakachi Y, Nakahara F, Nakamura T, Nakamura Y, Nakazato K, van Nimwegen E, Ninomiya N, Nishiyori H, Noma S, Noma S, Noazaki T, Ogishima S, Ohkura N, Ohimiya H, Ohno H, Ohshima M, Okada-Hatakeyama M, Okazaki Y, Orlando V, Ovchinnikov DA, Pain A, Passier R, Patrikakis M, Persson H, Piazza S, Prendergast JG, Rackham OJ, Ramilowski JA, Rashid M, Ravasi T, Rizzu P, Roncador M, Roy S, Rye MB, Saijyo E, Sajantila A, Saka A, Sakaguchi S, Sakai M, Sato H, Savvi S, Saxena A, Schneider C, Schultes EA, Schulze-Tanzil GG, Schwegmann A, Sengstag T, Sheng G, Shimoji H, Shimoni Y, Shin JW, Simon C, Sugiyama D, Sugiyama T, Suzuki M, Suzuki N, Swoboda RK, 't Hoen PA, Tagami M, Takahashi N, Takai J, Tanaka H, Tatsukawa H, Tatum Z, Thompson M, Toyodo H, Toyoda T, Valen E, van de Wetering M, van den Berg LM, Verado R, Vijayan D, Vorontsov IE, Wasserman WW, Watanabe S, Wells CA, Winteringham LN, Wolvetang E, Wood EJ, Yamaguchi Y, Yamamoto M, Yoneda M, Yonekura Y, Yoshida S, Zabierowski SE, Zhang PG, Zhao X, Zucchelli S, Summers KM, Suzuki H, Daub CO, Kawai J, Heutink P, Hide W, Freeman TC, Lenhard B, Bajic VB, Taylor MS, Makeev VJ, Sandelin A, Hume DA, Carninci P, Hayashizaki Y. A promoter-level mammalian expression atlas. *Nature*. 2014;507:462–470.
17. St Laurent G, Vyatkin Y, Antonets D, Ri M, Qi Y, Saik O, Shtokalo D, de Hoon MJ, Kawaji H, Itoh M, Lassmann T, Arner E, Forrest AR; Consortium F, Nicolas E, McCaffrey TA, Carninci P, Hayashizaki Y, Wahlestedt C, Kapranov P. Functional annotation of the vlinc class of non-coding RNAs using systems biology approach. *Nucleic Acids Res*. 2016;44:3233–3252.
18. Zhang H, Xue C, Shah R, Bermingham K, Hinkle CC, Li W, Rodrigues A, Tabita-Martinez J, Millar JS, Cuchel M, Pashos EE, Liu Y, Yan R, Yang W, Gosai SJ, VanDorn D, Chou ST, Gregory BD, Morrisey EE, Li M, Rader DJ, Reilly MP. Functional analysis and transcriptomic profiling of iPSC-derived macrophages and their application in modeling Mendelian disease. *Circ Res*. 2015;117:17–28.
19. Lin J, Hu Y, Nunez S, Foulkes AS, Cieply B, Xue C, Gerelus M, Li W, Zhang H, Rader DJ, Musunuru K, Li M, Reilly MP. Transcriptome-wide analysis reveals modulation of human macrophage inflammatory phenotype through alternative splicing. *Arterioscler Thromb Vasc Biol*. 2016;36:1434–1447.
20. Ballantyne RL, Zhang X, Nunez S, Xue C, Zhao W, Reed E, Salaheen D, Foulkes AS, Li M, Reilly MP. Genome-wide interrogation reveals hundreds of long intergenic noncoding RNAs that associate with cardiometabolic traits. *Hum Mol Genet*. 2016;25:3125–3141.
21. Saeed S, Quintin J, Kerstens HH, Rao NA, Aghajanirefah A, Matarese F, Cheng SC, Ratter J, Berentsen K, van der Ent MA, Sharifi N, Janssen-Megens EM, Ter Huurne M, Mandoli A, van Schaik T, Ng A, Burden F, Downes K, Frontini M, Kumar V, Giamarellos-Bourboulis EJ, Ouwehand WH, van der Meer JW, Joosten LA, Wijmenga C, Martens JH, Xavier RJ, Logie C, Netea MG, Stunnenberg HG. Epigenetic programming of monocyte-to-macrophage differentiation and trained innate immunity. *Science*. 2014;345:1251086.
22. Pham TH, Benner C, Lichtinger M, Schwarzfischer L, Hu Y, Andreesen R, Chen W, Rehli M. Dynamic epigenetic enhancer signatures reveal key transcription factors associated with monocytic differentiation states. *Blood*. 2012;119:e161–e171.
23. Xue C, Zhang X, Zhang H, Ferguson JF, Wang Y, Hinkle C, Li M, Reilly MP. De novo RNA sequence assembly during in vivo inflammatory stress reveals hundreds of unannotated lincRNAs in human blood CD14+ monocytes and in adipose tissue. *Physiol Genomics*. 2017;49:287–305. DOI: 10.1152/physiolgenomics.00001.02017.
24. Trapnell C, Roberts A, Goff L, Pertea G, Kim D, Kelley DR, Pimentel H, Salzberg SL, Rinn JL, Pachter L. Differential gene and transcript expression analysis of RNA-seq experiments with Tophat and Cufflinks. *Nat Protoc*. 2012;7:562–578.
25. Alvarez-Dominguez JR, Bai Z, Xu D, Yuan B, Lo KA, Yoon MJ, Lim YC, Knoll M, Slavov N, Chen S, Chen P, Lodish HF, Sun L. De novo reconstruction of adipose tissue transcriptomes reveals long non-coding RNA regulators of brown adipocyte development. *Cell Metab*. 2015;21:764–776.
26. Ramirez F, Dundar F, Diehl S, Gruning BA, Manke T. Deeptools: a flexible platform for exploring deep-sequencing data. *Nucleic Acids Res*. 2014;42:W187–W191.
27. Welter D, MacArthur J, Morales J, Burdett T, Hall P, Junkins H, Klemm A, Flicek P, Manolio T, Hindorff L, Parkinson H. The NHGRI GWAS catalog, a curated resource of SNP-trait associations. *Nucleic Acids Res*. 2014;42:D1001–D1006.
28. Altshuler DM, Gibbs RA, Peltonen L, Altshuler DM, Gibbs RA, Peltonen L, Dermitzakis E, Schaffner SF, Yu F, Peltonen L, Dermitzakis E, Bonnen PE, Altshuler DM, Gibbs RA, de Bakker PI, Deloukas P, Gabriel SB, Gwilliam R, Hunt S, Inouye M, Jia X, Palotie A, Parkin M, Whittaker P, Yu F, Chang K, Hawes A, Lewis LR, Ren Y, Wheeler D, Gibbs RA, Muzny DM, Barnes C, Darvishi K, Hurles M, Korn JM, Kristiansson K, Lee C, McCarrol SA, Nemesh J, Dermitzakis E, Keinan A, Montgomery SB, Pollack S, Price AL, Soranzo N, Bonnen PE, Gibbs RA, Gonzaga-Jauregui C, Keinan A, Price AL, Yu F, Anttila V, Brodeur W, Daly MJ, Leslie S, McVean G, Moutsianas L, Nguyen H, Schaffner SF, Zhang Q, Ghori MJ, McGinnis R, McLaren W, Pollack S, Price AL, Schaffner SF, Takeuchi F, Grossman SR, Shlyakhter I, Hostetter EB, Sabeti PC, Adebamowo CA, Foster MW, Gordon DR, Licinio J, Manca MC, Marshall PA, Matsuda I, Ngare D, Wang VO, Reddy D, Rotimi CN, Royal CD, Sharp RR, Zeng C, Brooks LD, McEwen JE. Integrating common and rare genetic variation in diverse human populations. *Nature*. 2010;467:52–58.
29. Benjamini Y, Yekutieli D. The control of the false discovery rate in multiple testing under dependency. *Ann Stat*. 2001;29:1165–1188.
30. Qian J, Nunez S, Reed E, Reilly MP, Foulkes AS. A simple test of class-level genetic association can reveal novel cardiometabolic trait loci. *PLoS One*. 2016;11:e0148218.
31. Harrow J, Frankish A, Gonzalez JM, Tapanari E, Diekhans M, Kokocinski F, Aken BL, Barrell D, Zadissa A, Searle S, Barnes I, Bignell A, Boychenko V, Hunt T, Kay M, Mukherjee G, Rajan J, Despacio-Reyes G, Saunders G, Steward C, Harte R, Lin M, Howald C, Tanzer A, Derrien T, Chrast J, Walters N, Balasubramanian S, Pei B, Tress M, Rodriguez JM, Ezkurdia I, van Baren J, Brent M, Haussler D, Kellis M, Valencia A, Reymond A, Gerstein M, Guigo R, Hubbard TJ. GENCODE: the reference human genome annotation for the ENCODE project. *Genome Res*. 2012;22:1760–1774.
32. Haerty W, Ponting CP. Unexpected selection to retain high GC content and splicing enhancers within exons of multiexonic lncRNA loci. *RNA*. 2015;21:333–346.
33. Sun K, Chen X, Jiang P, Song X, Wang H, Sun H. iSeeRNA: identification of long intergenic non-coding RNA transcripts from transcriptome sequencing data. *BMC Genomics*. 2013;14(suppl 2):S7.
34. Finn RD, Mistry J, Tate J, Coggill P, Heger A, Pollington JE, Gavin OL, Gunasekaran P, Ceric G, Forslund K, Holm L, Sonnhammer EL, Eddy SR, Bateman A. The Pfam protein families database. *Nucleic Acids Res*. 2010;38:D211–D222.
35. Lin MF, Jungreis I, Kellis M. PhyloCSF: a comparative genomics method to distinguish protein coding and non-coding regions. *Bioinformatics*. 2011;27:i275–i282.
36. Ulitsky I. Evolution to the rescue: using comparative genomics to understand long non-coding RNAs. *Nat Rev Genet*. 2016;17:601–614.

37. Camacho C, Coulouris G, Avagyan V, Ma N, Papadopoulos J, Bealer K, Madden TL. BLAST+: architecture and applications. *BMC Bioinformatics*. 2009;10:421.

38. Lam MT, Li W, Rosenfeld MG, Glass CK. Enhancer RNAs and regulated transcriptional programs. *Trends Biochem Sci*. 2014;39:170–182.

39. Ilott NE, Heward JA, Roux B, Tsitsiou E, Fenwick PS, Lenzi L, Goodhead I, Hertz-Fowler C, Heger A, Hall N, Donnelly LE, Sims D, Lindsay MA. Long non-coding RNAs and enhancer RNAs regulate the lipopolysaccharide-induced inflammatory response in human monocytes. *Nat Commun*. 2014;5:3979.

40. Marques AC, Hughes J, Graham B, Kowalczyk MS, Higgs DR, Ponting CP. Chromatin signatures at transcriptional start sites separate two equally populated yet distinct classes of intergenic long noncoding RNAs. *Genome Biol*. 2013;14:R131.

41. Kottgen A, Albrecht E, Teumer A, Vitart V, Krumsiek J, Hundertmark C, Pistis G, Ruggiero D, O'Seaghdha CM, Haller T, Yang Q, Tanaka T, Johnson AD, Kutalik Z, Smith AV, Shi J, Struchalin M, Middelberg RP, Brown MJ, Gaffo AL, Pirastu N, Li G, Hayward C, Zemunik T, Huffman J, Yengo L, Zhao JH, Demirkan A, Feitosa MF, Liu X, Malerba G, Lopez LM, van der Harst P, Li X, Kleber ME, Hicks AA, Nolte IM, Johansson A, Murgia F, Wild SH, Bakker SJ, Peden JF, Dehghan A, Steri M, Tenesa A, Lagou V, Salo P, Mangino M, Rose LM, Lehtimaki T, Woodward OM, Okada Y, Tin A, Muller C, Oldmeadow C, Putku M, Czamara D, Kraft P, Frogheri L, Thun GA, Grotevendt A, Gislason GK, Harris TB, Launer LJ, McArdle P, Shuldiner AR, Boerwinkle E, Coresh J, Schmidt H, Schallert M, Martin NG, Montgomery GW, Kubo M, Nakamura Y, Tanaka T, Munroe PB, Samani NJ, Jacobs DR Jr, Liu K, D'Adamo P, Ulivi S, Rotter JI, Psaty BM, Vollenweider P, Waeber G, Campbell S, Devuyst O, Navarro P, Kolcic I, Hastie N, Balkau B, Froguel P, Esko T, Salumets A, Khaw KT, Langenberg C, Wareham NJ, Isaacs A, Kraja A, Zhang Q, Wild PS, Scott RJ, Holliday EG, Org E, Viigimaa M, Bandinelli S, Metter JE, Lupo A, Trabetti E, Sorice R, Doring A, Lattka E, Strauch K, Theis F, Waldenberger M, Wichmann HE, Davies G, Gow AJ, Bruinenberg M, Stolk RP, Kooner JS, Zhang W, Winkelmann BR, Boehm BO, Lucae S, Penninx BW, Smit JH, Curhan G, Mudgal P, Plenge RM, Portas L, Persico I, Kirin M, Wilson JF, Mateo Leach I, van Gilst WH, Goel A, Ongen H, Hofman A, Rivadeneira F, Uitterlinden AG, Imboden M, von Eckardstein A, Cucca F, Nagaraja R, Piras MG, Nauck M, Schurmann C, Budde K, Ernst F, Farrington SM, Theodoratou E, Prokopenko I, Stumvoll M, Jula A, Perola M, Salomaa V, Shin SY, Spector TD, Sala C, Ridker PM, Kahonen M, Viikari J, Hengstenberg C, Nelson CP, Meschia JF, Nalls MA, Sharma P, Singleton AB, Kamatani N, Zeller T, Burnier M, Attia J, Laan M, Klopp N, Hillege HL, Kloiber S, Choi H, Pirastu M, Tore S, Probst-Hensch NM, Volzke H, Gudnason V, Parsa A, Schmidt R, Whitfield JB, Fornage M, Gasparini P, Siscovick DS, Polasek O, Campbell H, Rudan I, Bouatia-Naji N, Metspalu A, Loos RJ, van Duijn CM, Borecki IB, Ferrucci L, Gambaro G, Deary IJ, Wolffenbuttel BH, Chambers JC, Marz W, Pramstaller PP, Snieder H, Gyllensten U, Wright AF, Navis G, Watkins H, Witteman JC, Sanna S, Schipf S, Dunlop MG, Tonjes A, Ripatti S, Soranzo N, Toniolo D, Chasman DI, Raitakari O, Kao WH, Ciullo M, Fox CS, Caulfield M, Bochud M, Gieger C. Genome-wide association analyses identify 18 new loci associated with serum urate concentrations. *Nat Genet*. 2013;45:145–154.

42. Choi SH, Ruggiero D, Sorice R, Song C, Nutile T, Vernon Smith A, Concas MP, Traglia M, Barbieri C, Ndiaye NC, Stathopoulou MG, Lagou V, Maestrale GB, Sala C, Debette S, Kovacs P, Lind L, Lamont J, Fitzgerald P, Tonjes A, Gudnason V, Toniolo D, Pirastu M, Bellenguez C, Vasan RS, Ingelsson E, Leutenegger AL, Johnson AD, DeStefano AL, Visvikis-Siest S, Seshadri S, Ciullo M. Six novel loci associated with circulating VEGF levels identified by a meta-analysis of genome-wide association studies. *PLoS Genet*. 2016;12:e1005874.

43. Rubinow KB, Wall VZ, Nelson J, Mar D, Bomsztyk K, Askari B, Lai MA, Smith KD, Han MS, Vivekanandan-Giri A, Pennathur S, Albert CJ, Ford DA, Davis RJ, Bornfeldt KE. Acyl-CoA synthetase 1 is induced by Gram-negative bacteria and lipopolysaccharide and is required for phospholipid turnover in stimulated macrophages. *J Biol Chem*. 2013;288:9957–9970.

44. Abecasis GR, Auton A, Brooks LD, DePristo MA, Durbin RM, Handsaker RE, Kang HM, Marth GT, McVean GA. An integrated map of genetic variation from 1,092 human genomes. *Nature*. 2012;491:56–65.

45. Su X, Yu Y, Zhong Y, Giannopoulou EG, Hu X, Liu H, Cross JR, Ratsch G, Rice CM, Ivashkiv LB. Interferon-gamma regulates cellular metabolism and mRNA translation to potentiate macrophage activation. *Nat Immunol*. 2015;16:838–849.

46. Rocha VZ, Folco EJ, Sukhova G, Shimizu K, Gotsman I, Vernon AH, Libby P. Interferon-gamma, a Th1 cytokine, regulates fat inflammation: a role for adaptive immunity in obesity. *Circ Res*. 2008;103:467–476.

47. Wang P, Xue Y, Han Y, Lin L, Wu C, Xu S, Jiang Z, Xu J, Liu Q, Cao X. The STAT3-binding long noncoding RNA lnc-DC controls human dendritic cell differentiation. *Science*. 2014;344:310–313.

48. Nazari-Jahantigh M, Wei Y, Noels H, Akhtar S, Zhou Z, Koenen RR, Heyll K, Gremse F, Kiessling F, Grommes J, Weber C, Schober A. MicroRNA-155 promotes atherosclerosis by repressing Bcl6 in macrophages. *J Clin Invest*. 2012;122:4190–4202.

49. Li K, Ching D, Luk FS, Raffai RL. Apolipoprotein E enhances microRNA-146a in monocytes and macrophages to suppress nuclear factor-kappaB-driven inflammation and atherosclerosis. *Circ Res*. 2015;117:e1–e11.

50. Holdt LM, Beutner F, Scholz M, Gielen S, Gabel G, Bergert H, Schuler G, Thiery J, Teupser D. ANRIL expression is associated with atherosclerosis risk at chromosome 9p21. *Arterioscler Thromb Vasc Biol*. 2010;30:620–627.

51. Castellanos-Rubio A, Fernandez-Jimenez N, Kratchmarov R, Luo X, Bhagat G, Green PH, Schneider R, Kiledjian M, Bilbao JR, Ghosh S. A long noncoding RNA associated with susceptibility to celiac disease. *Science*. 2016;352:91–95.

52. Ding Q, Regan SN, Xia Y, Oostrom LA, Cowan CA, Musunuru K. Enhanced efficiency of human pluripotent stem cell genome editing through replacing TALENs with CRISPRs. *Cell Stem Cell*. 2013;12:393–394.

53. Hon CC, Ramilowski JA, Harshbarger J, Bertin N, Rackham OJ, Gough J, Denisenko E, Schmeier S, Poulsen TM, Severin J, Lizio M, Kawaji H, Kasukawa T, Itoh M, Burroughs AM, Noma S, Djebali S, Alam T, Medvedeva YA, Testa AC, Lipovich L, Yip CW, Abugessaisa I, Mendez M, Hasegawa A, Tang D, Lassmann T, Heutink P, Babina M, Wells CA, Kojima S, Nakamura Y, Suzuki H, Daub CO, de Hoon MJ, Arner E, Hayashizaki Y, Carninci P, Forrest AR. An atlas of human long non-coding RNAs with accurate 5′ ends. *Nature*. 2017;543:199–204.

54. Cui H, Xie N, Tan Z, Banerjee S, Thannickal VJ, Abraham E, Liu G. The human long noncoding RNA lnc-IL7R regulates the inflammatory response. *Eur J Immunol*. 2014;44:2085–2095.

55. Yang L, Duff MO, Graveley BR, Carmichael GG, Chen LL. Genomewide characterization of non-polyadenylated RNAs. *Genome Biol*. 2011;12:R16.

SUPPLEMENTAL MATERIAL

Data S1.

Detailed Methods

All human protocols for this work were approved by the University of Pennsylvania and Columbia University Medical Center Human Subjects Research Institutional Review Boards.

Isolation of human PBMC, CD14$^+$ monocytes and T cells
Peripheral blood mononuclear cells (PBMC) from peripheral blood were collected using BD VACUTAINER® CPT™ Cell Preparation Tubes with Sodium Citrate or gradient centrifugation in Ficoll (GE: Ficoll®-Paque Premium).[1] Monocytes were isolated from peripheral blood using CD14 MicroBeads for the positive selection of CD14$^+$ monocytes (MACS Milteny Biotech, Cat# 130-050-201) according to the manufacture protocol. Additional human PBMCs, monocytes and CD3$^+$ T cells for functional validation were obtained from de-identified healthy apheresis donors (demographic information not available) through the University of Pennsylvania's Human Immunology Core.

Differentiation of PBMC and monocytes-derived macrophage (HMDM) Isolated PBMCs or monocytes were cultured in macrophage culture media containing 20% fetal bovine serum in RPMI 1640 media supplemented with 100 ng/mL M-CSF (PeproTech, Cat# 300-25), for 7 days on BD Primaria™ tissue culture plate to induce macrophage differentiation as we described.[1]

Subject-specific iPSCs derivation, culture and maintenance Generation and characterization of subject-specific induced pluripotent stem cells (iPSCs) were performed by the iPSC Core Facility at Penn's Institute of Regenerative Medicine. iPSCs were derived from PBMCs using Sendai viral vectors as described.[1]

Differentiations of human iPSCs-derived macrophages (IPSDM) Detailed protocols were described in our recent publication.[1] Briefly, to induce differentiation, embryoid bodies were generated by culturing small aggregates of feeder-depleted iPSCs in COSTAR ultra-low attachment surface multiwell plate in StemPro-34 media supplemented with different cytokine cocktails. From day-8, macrophage culture media was used to enrich for myeloid precursors. At day-15, single cells were transferred to BD Primaria™ tissue culture plate for expansion and maturation, completed at day-22.

HMDM and IPSDM activation Macrophage activation was induced by 18-20h incubation with 20 ng/mL IFN-γ and 100 ng/mL LPS for M1-like activation, or 20 ng/mL IL-4 for M2-like activation.[1]

RNA-seq library preparation and sequencing As we described,[1, 2] RNA samples were extracted using All Prep DNA/RNA/miRNA Universal Kit (Qiagen, Valencia, CA). With a minimum of 300 ng input RNA, libraries were prepared using the ruSeq RNA Library Prep Kit v2 (RS-122-2101, Illumina, San Diego, CA) according to the manufacturer's protocol with the following modification: 1) the fragmentation time was decreased from 8 to 6 min to ensure libraries were > 100bp long and 2) PCR amplification was limited to 12 cycles for library enrichment to avoid bias from PCR "jackpot" mutations. Library length and concentration were evaluated with the Agilent 2100 Bioanalyzer and PCR quantification (KAPA) and pooled at 2 nM for massively parallel sequencing (2 x 100 bp) performed on an Illumina's HiSeq 2000.[1, 2] On average, in macrophage samples we obtained ~130 million filtered reads per sample with >95% mapping rate and in monocyte samples ~280 million filtered reads per sample with >93% mapping rate.

Alignment of RNA-seq reads and *de novo* assembly As we described,[17, 57] RNA-seq reads were aligned to the hg19 reference genome using STAR 2.3.0e[3] with default options. Analyses were based on filtered alignment files. *De novo* assembly was performed on merged alignment from HMDM M0, M1 and M2 using Cufflinks 2.1.1.[4] Transcripts that were at least 200 bp long and with at least 2 exons were kept for downstream analyses. We filtered transcripts that had exonic overlap with the following annotation: 1) known coding genes from RefSeq, GENCODE and UCSC; 2) microRNA, tRNA, snoRNA and rRNA from GENCODE; 3) pseudogenes from GENCODE, Gerstein group[5] and Vega.[6] Coding potential was assessed by iSeeRNA and HMMER-3[7] based on Pfam 27.0.[8] To define novel macrophage lincRNAs, we filtered the above lincRNAs that overlapped known lincRNA annotation from 1) RefSeq noncoding genes with "NR" prefix; 2) GENCODE noncoding RNAs; 3) lincRNAs from Ballantyne et al.;[9] 4) Ensembl noncoding RNAs; 5) lincRNAs from Cabili *et al.;*[10] 6) MiTranscriptome;[11] 7) lincRNAs from Ranzani et al.[12] LincRNAs were also filtered if the ±1kb extension had at least 10 reads in > 50% subjects and the extension overlaps the above annotation. Newly annotated lincRNAs were given default names from Cufflinks beginning with "CUFF". RNA-seq data are available from the NCBI Gene Expression Omnibus (GEO) under the accession number GSE55536.[1]

RNA-seq data analysis and bioinformatics The overall workflow is shown in **Figure 1**. Transcript abundance was measured in FPKM using Cufflinks 2.1.1.[4] Differential expression was tested with Cuffdiff, using annotation from RefSeq coding genes, GENCODE V19 lincRNAs, Cabili set lincRNAs and assembled lincRNAs. LincRNAs with an FDR-adjusted *P* value <0.01 and a fold change >2 were considered DE. Multi-dimensional scaling (MDS) was done with Euclidean distance based on $\log_{10}$ (FPKM + 0.1) using R programming.[11] Cannonical pathway analysis and network analysis were performed using Ingenuity Pathway Analysis software (Qiagen).

Coding potential filtering

Coding potential assessment was initially performed with iSeeRNA[13] and HMMER-3 on Pfam[14] on newly annotated macrophage lincRNAs. To further validate the effectiveness of coding potential assessment and perform additional coding potential filtering on the annotated lincRNA datasets, we applied PhyloCSF,[15] another widely used coding potential assessment tool to both annotated and newly annotated macrophage lincRNAs. For each lincRNA transcript, PhyloCSF was run on multiple sequence alignment of 29 mammalian genomes to identify ORFs in all three frames. A lincRNA was classified as coding if any of its transcripts had a score ≥100. The score cutoff of 100 was chosen to optimize the balance of false negative vs. false positive rates.[10]

Conservation and synteny analysis Many functional lincRNAs are known to have synteny (genomic regions flanked by homologous protein-coding genes)[16] despite low sequence similarity across species.[17-19] We examined the synteny of 2,766 macrophage lincRNAs in mouse using HomoloGene release 68 (http://www.ncbi.nlm.nih.gov/homologene) as previously described.[20] The neighboring genes of lincRNAs in human were identified, and the homologous genes were searched in HomoloGene. If homologous genes in the mouse were found for the two nearest neighboring genes in the human, we considered the lincRNA syntenic. Syntenic lincRNAs were further sub-divided as annotated or not annotated in mouse, using GENCODE M4 annotation (http://www.gencodegenes.org/mouse_releases/4.html), to assess whether there were annotated mouse lincRNAs in syntenic regions. For syntenic lincRNAs, we evaluated their sequence conservation using BLASTN.[21] The human lincRNA sequence was queried against the mouse genome with an E-value cutoff of 1×10^{-10}. Any hits in the mouse within the syntenic region were

then searched in human with the same E-value cutoff. Sequences that passed the reciprocal steps were considered conserved.

Tissue enrichment of HMDM mRNAs and lincRNAs We estimated lincRNA and mRNA gene expression in M0-, M1- and M2-HMDM, and 16 tissues using Human BodyMap RNA-seq datasets.[10] For each lincRNA and mRNA, we calculated its fractional expression level in each tissue by dividing the FPKM value by total FPKM value across HMDMs and 16 tissues. e.g. The fractional expression level of a linRNA in M0-HMDM is calculated as "FPKM(M-HMDM) / [FPKM(M0-HMDM)+FPKM(tissue 1)+…+FPKM(tissue16)]". K-means clustering was applied to mRNA and lincRNA fractional expression values using Euclidean distance as described.[22]

Histone modification profile analysis Histone H3 lysine 4 monomethylation (H3K4me1),[23, 24] histone H3 lysine 4 trimethylation (H3K4me3),[23] and histone H3 lysine 27 acetylation (H3K27ac)[24] ChIP-seq datasets for human HMDM were downloaded from GSE31621[24] or GSE58310.[23] We selected 2,009 lincRNAs that were expressed in at least 50% M0 samples as well as 15,201 mRNAs expressed in at least 50% M0 samples. 1,632 lincRNAs and 14,606 mRNAs had H3K4me1 and H3K4me3 signals. Histone modification was quantified within ±1.5 kb of each mRNA or lincRNA TSS using computeMatrix from deepTools v1.5.11.[25] Histone modification was then visualized using heatmapper option from deepTools. The H3K4me1/H3K4me3 ratio was calculated by dividing the mean H3K4me1 signal by mean H3K4me3 signal within the ±1.5kb region.

Analysis of unidirectional and bidirectional transcription

Bidirectional transcription is defined as transcription that occurs on both the forward and reverse strands of DNA simultaneously. Analysis was performed as previously described.[26] We first summarized the number of RNA-seq reads at the region of ±1 kb of lincRNA TSS. A minimum number of 3 reads was used to define transcription. For the region with transcription: 1) If there is no coverage at the region between TSS and 1 kb upstream of the lincRNA TSS, or there is coverage but the strand is the same as the lincRNA strand, we classify a lincRNA as unidirectionally transcribed. If there is coverage and on the strand opposite to the lincRNA strand, we classify the lincRNA as a bidirectionally transcribed.

Transcription factor binding analysis We downloaded PU.1 and C/EBPβ peaks identified in human macrophages from GSE31621.[24] Peaks from two replicates for each were merged. We then mapped the merged peaks to ±2kb of each TSS and gene body and counted the number of lincRNAs with PU.1 and C/EBPβ binding in all the M0-HMDM lincRNAs.

Interrogation of Genomic Regions from Genome-Wide Association Study (GWAS)
First, to probe broadly whether macrophage lincRNAs may underlie disease associations, we explored the overlap of M0-, M1- and M2-HMDM enriched macrophage lincRNAs with known disease-associated variants using data from the comprehensive NHGRI GWAS Catalog.[27] SNP coordinates were lifted from hg38 to hg19. Trait-associated SNPs that reached significance level of $P < 1 \times 10^{-5}$ were extracted if they overlapped macrophage lincRNAs.

Second, because of the important role of macrophage activation in cardiometabolic disease, we interrogated SNPs within macrophage-expressed lincRNAs for their specific association with 13 cardiometabolic traits using large public GWAS meta-analysis summary datasets (**Table S2**). Briefly, 63,586 genotyped and imputed (HAPMAP[28]) SNPs were mapped to macrophage lincRNAs (±1kb) and interrogated using two analytic strategies for each trait of interest. First, the minimum *P* value (min*P*) for the corresponding SNPs within each lincRNA was reported and

considered significant if it met a Bonferroni-adjusted threshold of P <0.05, and the Bonferroni-corrected P values were adjusted for the number of SNPs within all macrophage lincRNAs.[29] Second, a class-based method Genetic Class Association Testing (GenCAT)[30] was also applied to test the overall impact of all the SNPs within the interrogated lincRNA region. Briefly, GenCAT uses the SNP-level meta-analysis test statistics across all SNPs within a single class (e.g., a lincRNA), as well as the size of the class and its unique correlation structure, to determine if it is statistically meaningful. A class was considered significant if it had a GenCAT P value that met a Bonferroni-corrected threshold (adjusted for the number of lincRNAs present in the given consortia) P <0.05. These analyses were conducted separately for each trait within consortia datasets. Significant lincRNAs (by either minP or class-based analysis) were further prioritized to only include those that contained the strongest SNP level P value in the region (±500kb of the lincRNA) or if it was in low linkage disequilibrium (r^2 <0.3; based on 1000Genomes CEU data[31]) with a stronger single SNP in the region, suggesting a significant independent signal at the lincRNA locus.

Quantitative real-time RT-PCR Total RNA was isolated using the miRNeasy kit and underwent on-column DNase treatment (Qiagen). Reverse transcription was performed from equal amounts of DNA-free RNA (300 ng) per sample using the High Capacity RNA to cDNA Master Mix kit (Applied Biosystems). Diluted cDNA was then used as input for quantitative RT-PCR analysis performed in a total volume of 10 μl on the QuantStudio 7 Flex Real-Time PCR System (Applied Biosystems) using SYBR green PCR mix (Bio-Rad). Primers were designed using NCBI and obtained from IDT and are listed in **Table S3**. The specificity of each amplified product was monitored through the use of melting curves at the end of each amplification reaction. Unless otherwise indicated, each transcript's cycle threshold (Ct) value was normalized to the *ACTB* Ct value for each sample, and a transcript's relative expression was determined through the $2^{-(\Delta\Delta Ct)}$ method.

Nuclear and cytoplasmic RNA fractionation As previously described,[20] for localization of lincRNAs prioritized for further study, HMDM cell pellet underwent subcellular fractionation using the NE-PER Nuclear and Cytoplasmic Extraction Kit (Thermo Fisher Scientific, Cat# 78833) with the addition of RNase inhibitor (Thermo Fisher Scientific, Cat# 10777019) to the lysis buffers. Total RNA was then isolated from each subcellular fraction using the miRNeasy kit (Qiagen). Quantitative real-time RT-PCR was performed for the lincRNAs in each fraction, with normalization of each fraction to the mean Ct of *U6* using *U6* snRNA Taqman microRNA assay (Thermo Fisher Scientific, Cat# 4427975) and *ACTB* combined. To ensure each subcellular fraction had only limited cross-contamination, relative *U6* and *ACTB* levels were measured separately to confirm their abundance in the nuclear and cytoplasmic compartments, respectively.

THP-1 cell culture

THP-1 human acute monocytic leukemia cell line was obtained from ATCC (ATCC® TIB-202™) and grown in suspension in in RPMI-1640 media supplemented with 10% FBS, 1 mM Sodium Pyruvate, 10 mM HEPES, and 50 μM 2-Mercaptoethanol. THP-1 macrophages were differentiated from THP-1 monocytic cell lines in THP-1 culture media supplemented with 100 nM Phorbol 12-myristate 13-acetate (PMA) for 3 days.

Knockdown of *MacORIS* in THP-1 derived macrophages (THP-1Φ) by ASO or siRNA

THP-1 monocytes were differentiated to THP-1Φ for 72 hours using 100 nM PMA. Knockdown of *MacORIS* were performed in THP-1Φ by transfection of single-stranded antisense oligonucleotides (ASO) or siRNA using Lipofectamine® RNAiMAX Transfection Reagent (Thermo Fisher Scientific, Cat# 13778150). ASOs targeting exon 2 of *MacORIS* were obtained from Exiqon and used at 10 nM. siRNA was obtained from Dharmacon and used at 50 nM. Cells were incubated with ASO or siRNA for 6 hours. Experiments were performed 48 hours after the ASO or siRNA treatment, and knockdown efficiency was confirmed for each individual experiment.

ASO sequence: AAGGATTTGAGTGATC
Control ASO sequence: AACACGTCTATACGC (Exiqon 300610, Batch 237122)

siRNA sequence:
sense – CCAAAUGAGAAACAAGAAAUU; anti-sense UUUCUUGUUUCUCAUUUGGUU
Control siRNA sequence: ON-TARGETplus Non-targeting Pool (Dharmacon D-001810-10-05)

Western blotting

Cells were lysed in RIPA buffer. Protein concentrations were assessed using BCA Protein Assay Kit (Pierce, Cat# 23225) and equal amounts of protein (20 µg) were separated by SDS-PAGE and transferred onto PVDF membranes. Protein expression was detected using the appropriate primary antibody: p-STAT1 (Tyr701) (Cell Signaling, Cat# 7649, 1:1000), p-JAK2 (Tyr1008) (Cell Signaling, Cat# 8082, 1:1000), STAT1 (Cell Signaling, Cat# 9172, 1:1000), JAK2 (Cell Signaling, Cat# 3230, 1:1000) and β-actin (Cell Signaling, Cat# 5125, 1:2000) and corresponding secondary antibodies (1:2000) to each primary antibodies used. Signals were visualized by SuperSignal™ West Pico Chemiluminescent Substrate (Thermo Fisher Scientific, Cat# 34080), and analyzed with an Amersham Imager 600 densitometer (GE Healthcare Life Sciences, Pittsburgh, PA) and quantified with Image J (http://rsbweb.nih.gov/ij/download.html). The densitometry values of the phosphorylated protein were first normalized to the respective total protein. The ratio of p-JAK2/JAK2 or p-STAT1/STAT1 for each sample was then normalized to the average of samples in the control group.

Flow cytometry analysis

THP-1Φ were dissociated using Cellstripper (Corning, Cat# 25-056-Cl), washed in staining buffer (BD, Cat# 554656), and blocked with 20 µl Fc-receptor antibodies for 10 min on ice, and then stained with PE anti-human CD119 (IFN-γ R α chain) antibody (Biolegend, Cat# 308703, 1:100 dilution from 400 µg/mL) at 4 µg/mL for 20 minutes on ice. The negative controls were stained using PE Mouse IgG1, κ Isotype Ctrl at 4 µg/mL (Biolegend, Cat# 400111, 1:50 dilution from a stock of 200 µg/mL). Samples were analyzed using BD LSRII flow cytometer (BD Biosciences, San Jose, CA). Cells were plotted according to forward scatter and side scatter profiles and gated to exclude cell doublets and debris. Data were analyzed by using FlowJo software (Tree Star, Ashland, OR).

In vitro* transcription and translation of *MacORIS

The Promega™ TNT™ Quick Coupled Transcription/Translation System (Cat# L1171) and transcend nonradioactive translation detection system was used to *in vitro* transcribe and translate the full-length *MacORIS* using the annotated sequence of *RP11-472N13.3* (ENST00000433770.1) from the T7 promoter of a pcDNA3.1+ plasmid. Products from

transcription/translation reactions were labeled with biotinylated lysine. 1 ul of the reaction products were added to 15 ul SDS sample buffer, heat denatured and resolved on a NuPage 4-12% SDS–polyacrylamide gel (Life Technologies). Protein products labeled with the biotinylated Transcend tRNA were detected with streptavidin antibody and Western Blue reagent using Transcend® nonradioactive translation detection system per the manufacturer's instructions. The luciferase T7 control plasmid supplied with the kit was used as the positive control.

Statistical analysis Specific analyses of RNA-seq and genomic data are described within each section. For analysis of gene ontology (GO) pathways in RNA-seq data, significant enrichment was declared at FDR adjusted *P* values <0.05 using Benjamini and Hochberg method.[32] Enrichment analysis was performed on DAVID using Biological Process category.[33] Non-sequencing data were analyzed with GraphPad Prism 6 (GraphPad Software, San Diego, CA). Data are presented as means ± SEM unless otherwise stated. Non-sequencing data were analyzed with GraphPad Prism 6 (GraphPad Software, San Diego, CA). Differences between two groups were assessed by Student's t tests (2-tailed). One-way analysis of variance (ANOVA) followed by Dunnett's test was used to correct for multiple comparisons. Results were declared significant if *P* values <0.05.

Accession codes RNA-seq data are available from the NCBI Gene Expression Omnibus (GEO) under the accession numbers GSE55536. Published H3K4me1 and H3K4me3 ChIP-seq datasets for human HMDM were from GSE58310.[23] PU.1 and C/EBPβ ChIP-seq datasets and H3K27ac ChIP-seq datasets in human HMDM were from GSE31621.[24] Published RNA-seq data of murine bone marrow derived macrophages were from GSE40978,[34] GSE38371,[35] and GSE58283.[36]

Table S1. Subject demographics of RNA-seq studies.

Subject	Sex	Race	Age	HMDM	IPSDM	iPSC	Monocyte
1	Male	Caucasian	25	1	1	1	
2	Male	Caucasian	65	1	1	1	
3	Male	Caucasian	29	2			
4	Female	Caucasian	28	1	1	1	
5	Female	Caucasian	45	2			
6	Female	Caucasian	30	1			
1272	Male	Caucasian	24				1
1352	Male	Caucasian	45				1
1416	Male	Caucasian	31				1
1482	Male	Caucasian	37				1
1072	Female	Caucasian	20				1
1484	Female	Caucasian	19				1

The numbers “1” and “2” in the table represent the number of biological replicates.

Table S2. Cardiometabolic traits evaluated in Genetics Consortia.

Consortium	Trait	# GWASs	# Individuals	# SNPs
CARDIoGRAM	Coronary artery disease (CAD)	22	86,995	2,420,350
DIAGRAM	Type 2 diabetes (T2D)	12	69,033	2,465,481
GIANT	Body mass indes (BMI)	80	123,865	2,471,506
	Height	61	183,727	2,469,625
	Waist-hip ratio adjusted for BMI	61	77,167	2,483,313
GLGC	HDL cholesterol	46	99,900	2,623,048
	LDL cholesterol	46	95,454	2,623,048
	Triglycerides	46	96,598	2,623,179
	Total cholesterol	46	100,184	2,623,032
MAGIC	Fasting glucose	21	46,186	2,470,468
	Fasting insulin	21	38,238	2,461,097
	HOMA-B	21	36,466	2,456,937
	HOMA-IR	21	37,037	2,458,065
	Hemoglobin A1C	23	46,368	2,562,524

Table S3. Primers for qRT-PCR validation.

LincRNA	Forward Primer Sequence (5' ➔ 3')	Reverse Primer Sequence (5' ➔ 3')
MIR155HG	TTGCAGGTTTTGGCTTGTTCA	CGTTACCTGGGGGAAAGTACC
RP11-10J5.1	GGAAACAGATGGGAACCTCA	CTGTCTTTGGACACCCACCT
CTB-41I6.2	ACCAGGGAAACCCCAAATGTC	AGTGGTGCCAAATGCTGTAGT
RP11-701P16.5	ACGTGGGCGTTTCTTTCTGT	AGCTGCTATCGCCAAGATCC
MIR146A	CCCACCCTTCTCACACTCTG	CCGATCTCTGGTGTCGGTTG
linc-HEATR6-2	CCTAGTCAAGGAACTCCAGACA	CCCTAAGATCGTCATCCCTTCC
linc-SLC39A10-10	GCCCACGTTTAGGAATGTCTC	TCCATGGAATGGGTATACCACCG
RP4-794H19.4	CTTTCCTGCTGGCTACATCAC	TAACACCAGAGCTGTAGAGGG
RP5-836N10.1	CACAGGCTGAGTTTGTGCTA	GAGGGTTCTTTCTCACCGCC
RP11-184M15.1	GCGGGATTGTCTGGTTTCAA	CATCCAGGACATGCCAGCTA
MacORIS	AGCGTTGGCTTTCCCCAAAT	GCCGCTAGTATTCAGCGAGA
ACTB	ACAGAGCCTCGCCTTTGCC	GATATCATCATCCATGGTGAGCTGG
TNFAIP3	CTTGTGGCGCTGAAAACGAA	CCATGGGTGTGTCTGTGGAA
TNF	CCTCAGCCTCTTCTCCTTCC	GGCTACAGGCTTGTCACTCG
IL1B	CTTCGAGGCACAAGGCACAA	TTCACTGGCGAGCTCAGGTA
SOCS1	CACGCACTTCCGCACATTC	TAAGGGCGAAAAAGCAGTTCC
SOCS3	CCTGCGCCTCAAGACCTTC	GTCACTGCGCTCCAGTAGAA

Table S4. Coding potential assessment of macrophage lincRNAs with PhyloCSF using score cutoff of 100. See Excel file.

Table S5. Annotation, expression, synteny, conservation, tissue enrichment and chromatin signature of macrophage lincRNAs. See Excel file.

Table S6. DE lincRNAs; Monocyte vs. M0-HMDM. See Excel file.

Table S7. Top enriched GO terms for the nearest protein coding genes to the up-regulated enhancer-associated lincRNAs in M1 activation. See Excel file.

Table S8. Top canonical pathways for the nearest protein coding genes to the up-regulated enhancer-associated lincRNAs in M1 activation. See Excel file.

Table S9. Top diseases and biological functions for the nearest coding genes to the up-regulated enhancer-associated lincRNAs in M1 activation. See Excel file.

Table S10. Fold change of enhancer-associated lincRNAs and their nearest coding genes up-regulated in M1-activation. See Excel file.

Table S11. DE lincRNAs; M0-HMDM vs. M1-HMDM and M0-IPSDM vs. M1-IPSDM. See Excel file.

Table S12. DE lincRNAs; M0-HMDM vs. M2-HMDM and M0-IPSDM vs. M2-IPSDM. See Excel file.

Table S13. Prioritized differentially expressed lincRNAs in M1- and M2-activation.

Position	LincRNA	Size (bp)	Exon #	Synteny	Enrichment			H3K4me1/ H3K4me3	HMDM					IPSDM				
					Fractional Expression				FPKM			Fold Change		FPKM			Fold Change	
					M0	M1	M2		M0	M1	M2	M0 vs. M1	M0 vs. M2	M0	M1	M2	M0 vs. M1	M0 vs. M2
M1-induced																		
chr21:26934221-26947480	MIR155HG	13260	4	0	0.34	0.69	0.39	0.5	4.57	21.45	5.62	4.70	1.23	1.51	23.73	1.81	15.76	1.20
chr6:138264216-138266939	RP11-10J5.1	2724	2	1	0.80	0.94	0.71	8.6	3.71	18.48	2.38	4.98	0.64	0.21	8.31	0.04	38.78	0.18
chr4:185765739-185776905	RP11-701P16.5	11167	3	1	0.42	0.91	0.39	3.9	2.28	43.70	2.11	19.21	0.93	0.10	14.04	0.13	134.01	1.28
chr17:8870840-8880312	CTB-41I6.2	9473	2	1	0.40	0.73	0.47	0.7	1.57	6.83	2.14	4.35	1.36	1.73	3.92	2.07	2.27	1.20
chr17:58160925-58166557	Linc-HEATR6-2	5633	4	2	0.27	0.91	0.37	5.3	16.15	432.48	27.23	26.77	1.69	3.55	86.38	3.59	24.31	1.01
chr2:192559982-192563100	Linc-SLC39A10-10	3119	2	2	0.35	0.72	0.40	6.7	6.01	27.46	7.20	4.57	1.20	3.56	28.05	11.17	7.87	3.13
chr5:159895275-159914433	MIR146A	19159	2	2	0.57	0.82	0.46	0.3	2.55	8.04	1.61	3.15	0.63	0.69	2.10	0.26	3.03	0.38
chr1:59486059-59510286	RP4-794H19.4	24228	4	2	0.25	0.76	0.34	3.4	1.66	18.64	2.76	11.21	1.66	1.88	17.03	3.14	9.06	1.67
M2-induced																		
chr4:129489127-129491686	RP11-184M15.1	2560	2	2	0.92	0.19	0.98	3.3	24.88	0.41	128.65	0.02	5.17	0.89	0.32	74.33	0.36	83.43
chr1:112142277-112151345	RP5-836N10.1	9069	5	1	0.32	0.20	0.72	1.0	1.25	0.72	7.92	0.58	6.36	1.74	1.39	5.47	0.80	3.14

Synteny: “0”, non-syntenic; “1”, syntenic but not annotated in mouse genome; “2”, syntenic and annotated in mouse genome.
Enrichment: LincRNAs with fractional expression of >0.2 are defined as “enriched” lincRNAs.

Table S14. Macrophage lincRNAs harbor genetic variants associated with traits in GWASs. See Excel file.

Table S15. QC summary of public datasets of RNA-seq of murine bone marrow-derived macrophages.

	Fastq	Reads mapped	Reads mapped and filtered
GSE40978	102,271,966	96,083,740	93,237,777
GSE38371	159,079,914	144,394,658	134,226,876
GSE58283	89,025,667	86,838,785	73,712,948

Table S16. DE lincRNAs; iPS vs. M0-IPSDM. See Excel file.

Table S17. DE lincRNAs; M0-HMDM vs. M0-IPSDM. See Excel file.

Table S18. Expression of DE lincRNAs between M0-HMDM and M0-IPSDM upon M1- and M2-activation. See Excel file.

Table S19. Comparison of DE lincRNAs in LPS-treated monocytes and M1-HMDM. See Excel file.

Table S20. Macrophage lincRNAs with FANTOM CAT lncRNA catalog annotation. See Excel file.

Figure S1. Correlation between biological replicates.

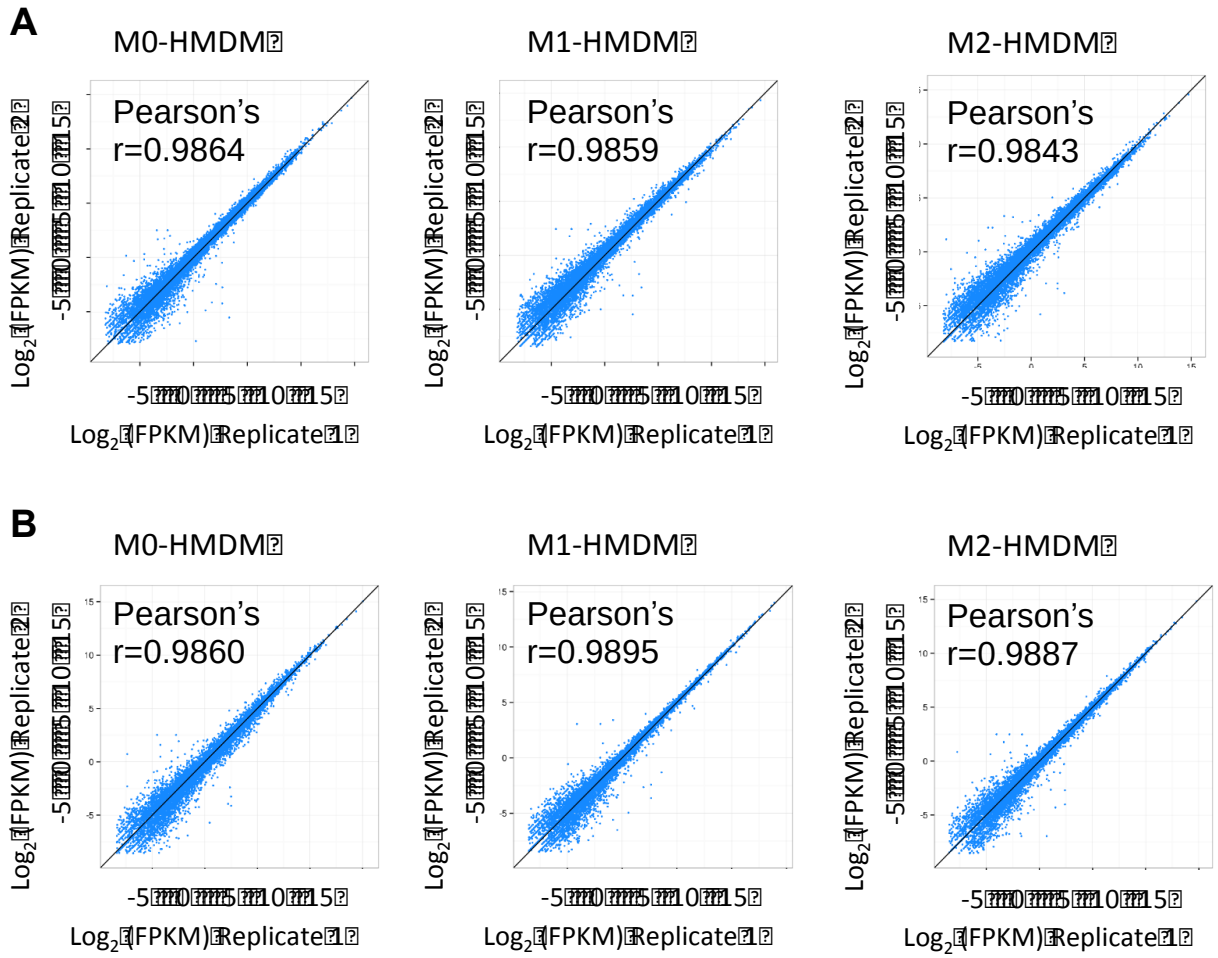

There was strong correlation of lincRNA expression between biological replicates (**A**. Subject 3 and **B**. Subject 5.). Pearson's correlation coefficients were depicted above each graph.

Figure S2. The “activation state”-specific lincRNAs were more likely to be previously unannotated lincRNAs.

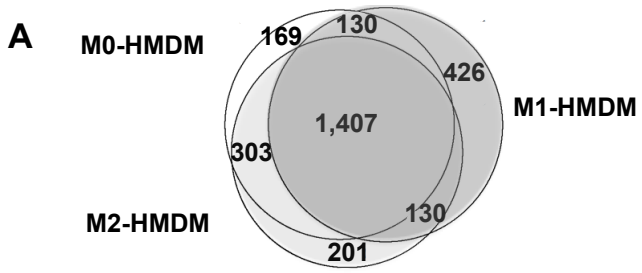

B **Number of newly annotated and known lincRNAs**

	Newly Annotated	Known
M1-specific lincRNAs	196	230
Non M1-specific lincRNAs	665	1675
P-value by Fisher’s exact test	2.58×10^{-12}	

C **Number of newly annotated and known lincRNAs**

	Newly Annotated	Known
M2-specific lincRNAs	85	116
Non M2-specific lincRNAs	776	1789
P-value by Fisher’s exact test	6.33×10^{-4}	

Among the 2,766 lincRNAs, over 50% (1,407) of the lincRNAs were expressed across M0-, M1-, and M2-HMDM activation states while a small percentage of lincRNAs were highly specific to either M0-, M1- or M2-HMDMs A small percentage of lincRNAs were highly specific to either M0-, M1- or M2-HMDMs (**A**). (**B**) and (**C**) Compared to the 861 newly annotated lincRNAs out of the 2,766 macrophage lincRNAs, there were 196 newly annotated lincRNAs out of 426 M1-specific lincRNAs ($P = 2.58 \times 10^{-12}$) and 85 newly annotated lincRNAs out of 201 M2-specific lincRNAs ($P = 6.33 \times 10^{-4}$) by Fisher’s exact test, underscoring the importance of interrogating lincRNAs within a cell-specific and functional context.

Figure S3. Characteristics of lincRNAs vs. protein coding genes.

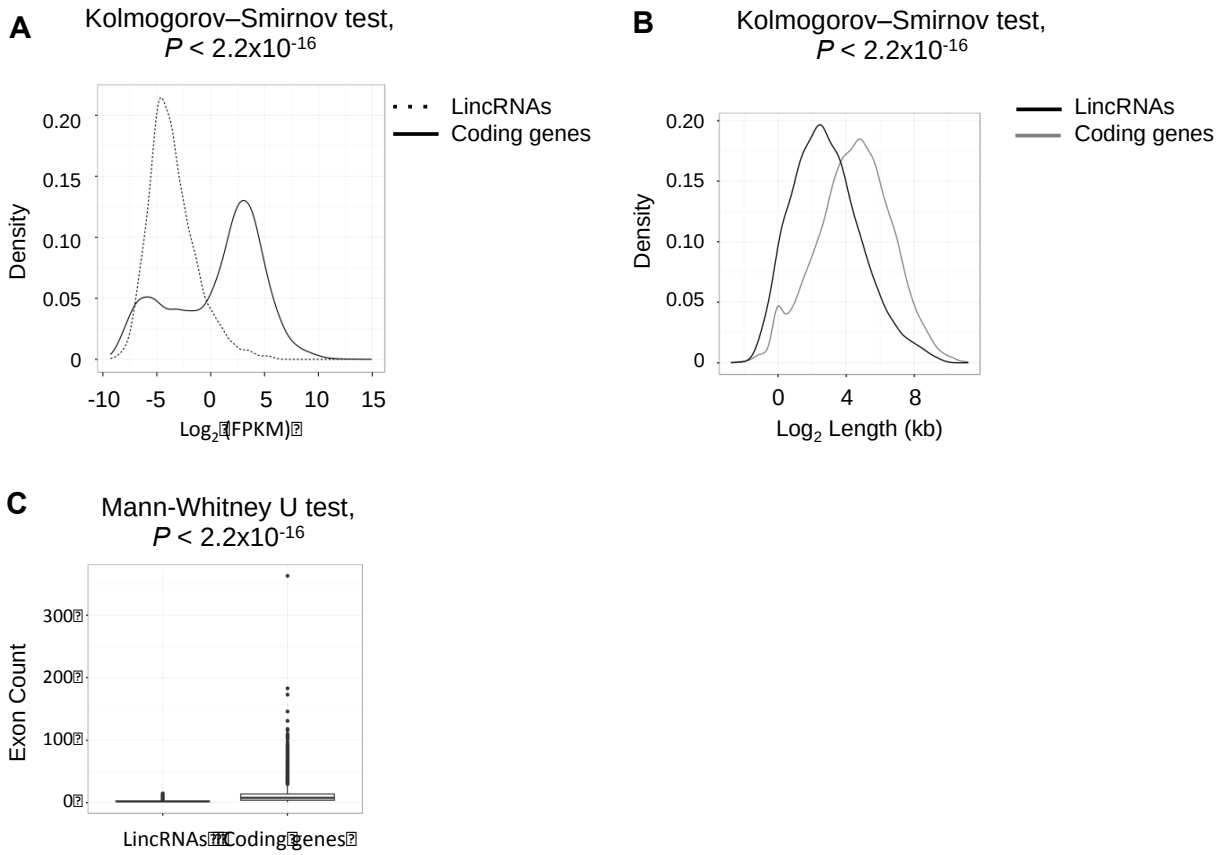

(A) Expression level distributions for lincRNAs and protein coding genes. **(B)** Distribution of the length of lincRNAs and protein coding genes. **(C)** Distribution of the number of exons in lincRNAs and protein coding genes. Kolmogorov–Smirnov test

Figure S4. Profound differentiation-induced lincRNA profile change from CD14⁺ monocytes to macrophages.

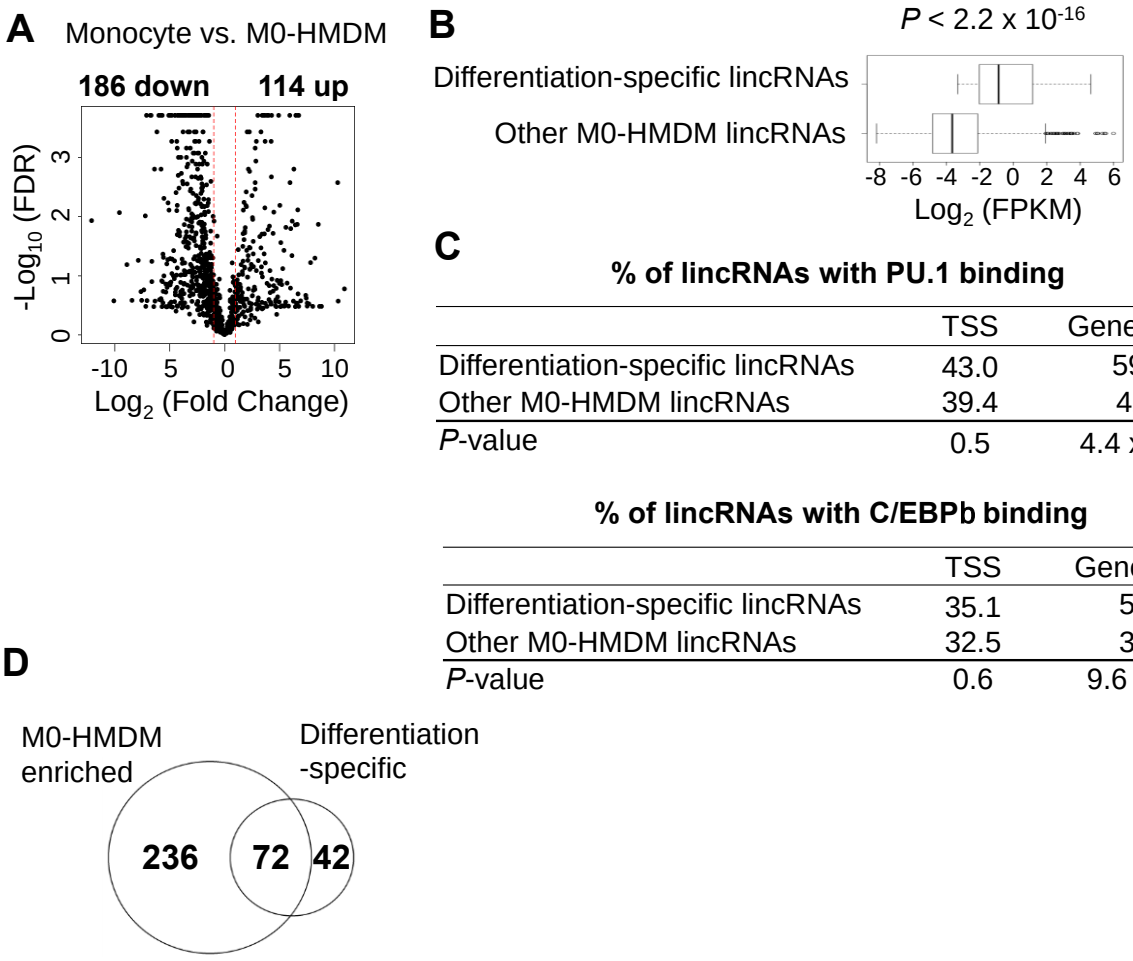

% of lincRNAs with PU.1 binding

	TSS	Gene Body
Differentiation-specific lincRNAs	43.0	59.6
Other M0-HMDM lincRNAs	39.4	42.4
P-value	0.5	4.4×10^{-4}

% of lincRNAs with C/EBPb binding

	TSS	Gene Body
Differentiation-specific lincRNAs	35.1	58.8
Other M0-HMDM lincRNAs	32.5	35.5
P-value	0.6	9.6×10^{-7}

(A) Using our RNA-seq dataset of CD14⁺ monocytes (age/race matched, n=6 subjects),[37] we identified differentially expressed lincRNAs during monocyte to M0-HMDM differentiation; compared to monocytes, 114 lincRNAs were up-regulated in M0-HMDM and 186 lincRNAs were down-regulated in M0-HMDM. **(B)** The up-regulated lincRNAs during macrophage differentiation showed more abundant expression than other M0-HMDM lincRNAs, and **(C)** demonstrated enriched PU.1 and C/EBPβ binding at gene body, but not TSS. **(D)** Venn diagram showed overlap between the 308 M0-HMDM-enriched lincRNAs and the 114 DE lincRNAs up-regulated during monocyte to M0-HMDM differentiation.

Figure S5. Characteristics of enhancer-associated lincRNAs and gene ontology and Ingenuity Pathway Analysis of the nearest protein coding genes to the up-regulated enhancer-associated lincRNAs during M1-activation.

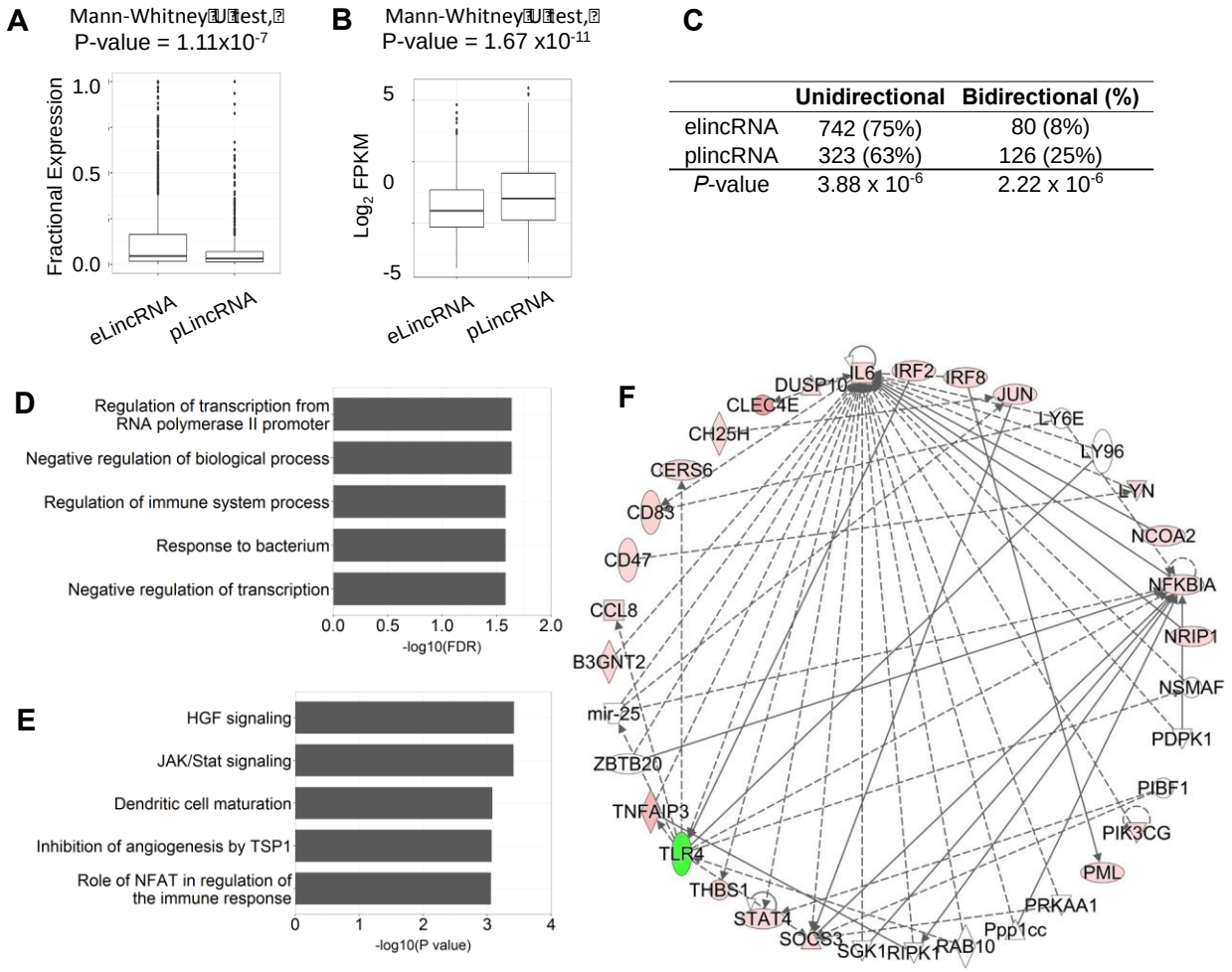

	Unidirectional	Bidirectional (%)
elincRNA	742 (75%)	80 (8%)
plincRNA	323 (63%)	126 (25%)
P-value	3.88 x 10^{-6}	2.22 x 10^{-6}

Polyadenylated enhancer-associated lincRNAs (elincRNAs) are more macrophage-enriche**d (A)**, less abundant **(B)**, and more likely to be a unidirectional transcript **(C)** compared with promoter-associated lincRNAs (plincRNAs). **(D)** Top 5 gene ontology (GO) terms enriched in the 194 nearest coding genes (expressed at FPKM > 1%) to the up-regulated enhancer-associated lincRNAs in M1-activation (see complete list in **Table S7**). **(E)** Top 5 canonical pathways in the nearest coding genes to the up-regulated enhancer lincRNAs in M1-activation (see complete list in **Table S8**). **(F)** Ingenuity Pathway Analysis using the nearest coding genes to the up-regulated enhancer-associated lincRNAs in M1-activation. The diagram reflects the regulatory networks, which show direct (solid line) and indirect (dash line) interactions between all the genes (red, up-regulated; green, down-regulated).

Figure S6. qRT-PCR validation and genome browser view of a newly annotated lincRNA *CUFF.15710*.

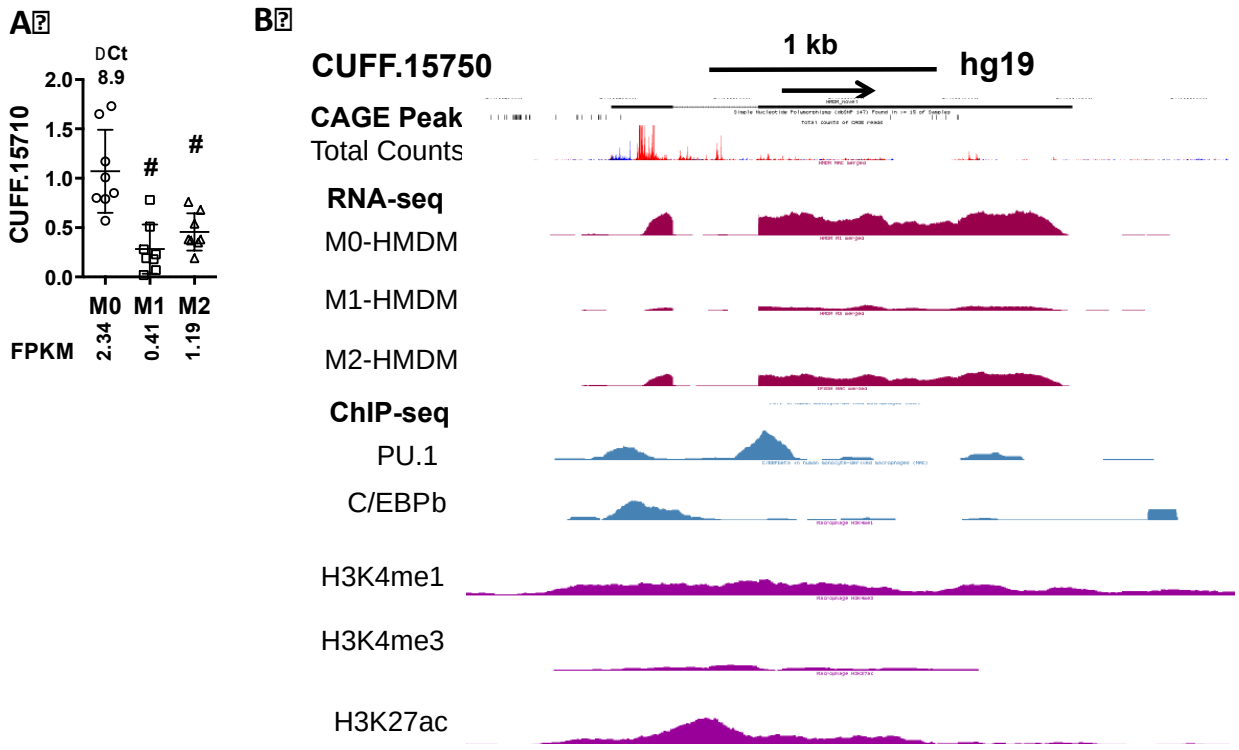

(A) One of the most abundantly expressed novel lincRNAs, *CUFF.15710*, was suppressed by both M1 and M2 activation. And the pattern was consistent between qRT-PCR and RNA-seq (**A & B**). (**B**) Genome browser view shows the lincRNA structure and exon/intron boundary by RNA-seq, CAGE peak defining transcription start site (TSS), PU.1 and C/EBPβ binding sites, and enhancer-like chromatin feature with weak H3K4me3 and strong H3K4me1 signals at the putative TSS.

Figure S7. *In vitro* transcription and translation of *MacORIS* and knock down of *MacORIS* by siRNA.

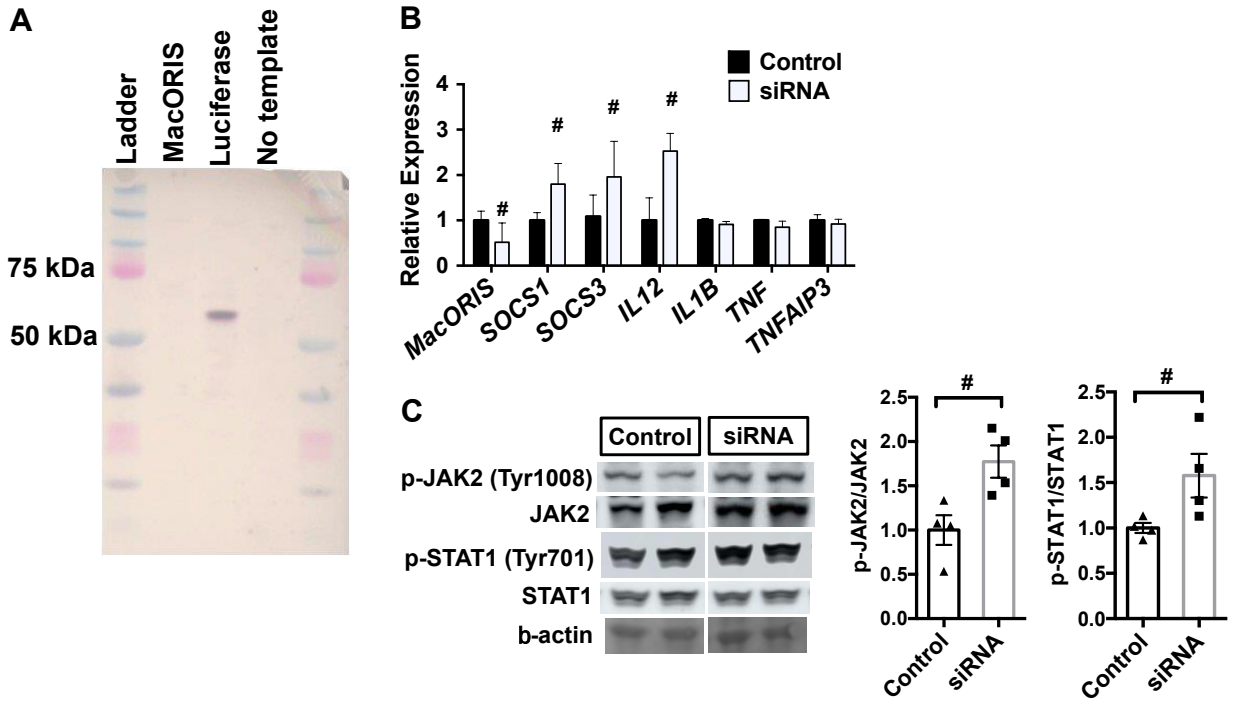

(**A**) *In vitro* transcription and translation of *MacORIS* did not produce any detectable peptides. (**B**) Knock down (KD) of *MacORIS* by siRNA in THP-1Φ enhanced expression of IFN-γ induced negative regulators *SOCS1* and *SOCS3*, but no effect on LPS-induced inflammatory genes such as *TNF*, *TNFAIP3 and IL1B.* (**C**) KD of *MacORIS* enhanced the phosphorylation of JAK2 and STAT1, generally consistent with the effects of KD by ASO as shown in **Figure 6**. The representative images shown in (**C**) were rearranged from the original capture by removing the gel segment between Control and siRNA groups. Space was inserted to disclose this manipulation. The representative images represent 2 experiments. The data from 4 independent experiments were quantified by ratio of densitometry of p-JAK2/JAK and p-STAT1/STAT1 and normalized to the Control group.

Supplemental References:

1. Zhang H, Xue C, Shah R, Bermingham K, Hinkle CC, Li W, Rodrigues A, Tabita-Martinez J, Millar JS, Cuchel M, Pashos EE, Liu Y, Yan R, Yang W, Gosai SJ, VanDorn D, Chou ST, Gregory BD, Morrisey EE, Li M, Rader DJ, Reilly MP. Functional analysis and transcriptomic profiling of ipsc-derived macrophages and their application in modeling mendelian disease. *Circulation research*. 2015;117:17-28
2. Liu Y, Ferguson JF, Xue C, Ballantyne RL, Silverman IM, Gosai SJ, Serfecz J, Morley MP, Gregory BD, Li M, Reilly MP. Tissue-specific rna-seq in human evoked inflammation identifies blood and adipose lincrna signatures of cardiometabolic diseases. *Arteriosclerosis, thrombosis, and vascular biology*. 2014;34:902-12.
3. Dobin A, Davis CA, Schlesinger F, Drenkow J, Zaleski C, Jha S, Batut P, Chaisson M, Gingeras TR. Star: Ultrafast universal rna-seq aligner. *Bioinformatics*. 2013;29:15-21
4. Trapnell C, Roberts A, Goff L, Pertea G, Kim D, Kelley DR, Pimentel H, Salzberg SL, Rinn JL, Pachter L. Differential gene and transcript expression analysis of rna-seq experiments with tophat and cufflinks. *Nature protocols*. 2012;7:562-578
5. Zhang Z, Carriero N, Zheng D, Karro J, Harrison PM, Gerstein M. Pseudopipe: An automated pseudogene identification pipeline. *Bioinformatics*. 2006;22:1437-1439
6. Wilming LG, Gilbert JG, Howe K, Trevanion S, Hubbard T, Harrow JL. The vertebrate genome annotation (vega) database. *Nucleic acids research*. 2008;36:D753-760
7. Finn RD, Clements J, Eddy SR. Hmmer web server: Interactive sequence similarity searching. *Nucleic acids research*. 2011;39:W29-37
8. Finn RD, Tate J, Mistry J, Coggill PC, Sammut SJ, Hotz HR, Ceric G, Forslund K, Eddy SR, Sonnhammer EL, Bateman A. The pfam protein families database. *Nucleic acids research*. 2008;36:D281-288
9. Ballantyne RL, Zhang X, Nunez S, Xue C, Zhao W, Reed E, Salaheen D, Foulkes AS, Li M, Reilly MP. Genome-wide interrogation reveals hundreds of long intergenic noncoding rnas that associate with cardiometabolic traits. *Human molecular genetics*. 2016;25:3125-3141.
10. Cabili MN, Trapnell C, Goff L, Koziol M, Tazon-Vega B, Regev A, Rinn JL. Integrative annotation of human large intergenic noncoding rnas reveals global properties and specific subclasses. *Genes & development*. 2011;25:1915-1927
11. Iyer MK, Niknafs YS, Malik R, Singhal U, Sahu A, Hosono Y, Barrette TR, Prensner JR, Evans JR, Zhao S, Poliakov A, Cao X, Dhanasekaran SM, Wu YM, Robinson DR, Beer DG, Feng FY, Iyer HK, Chinnaiyan AM. The landscape of long noncoding rnas in the human transcriptome. *Nature genetics*. 2015;47:199-208
12. Ranzani V, Rossetti G. The long intergenic noncoding rna landscape of human lymphocytes highlights the regulation of t cell differentiation by linc-maf-4. 2015;16:318-325
13. Sun K, Chen X, Jiang P, Song X, Wang H, Sun H. Iseerna: Identification of long intergenic non-coding rna transcripts from transcriptome sequencing data. *BMC genomics*. 2013;14 Suppl 2:S7
14. Finn RD, Mistry J, Tate J, Coggill P, Heger A, Pollington JE, Gavin OL, Gunasekaran P, Ceric G, Forslund K, Holm L, Sonnhammer EL, Eddy SR, Bateman A. The pfam protein families database. *Nucleic acids research*. 2010;38:D211-222
15. Lin MF, Jungreis I, Kellis M. Phylocsf: A comparative genomics method to distinguish protein coding and non-coding regions. *Bioinformatics*. 2011;27:i275-282
16. Ulitsky I, Bartel DP. Lincrnas: Genomics, evolution, and mechanisms. *Cell*. 2013;154:26-46

17. Hezroni H, Koppstein D, Schwartz MG, Avrutin A, Bartel DP, Ulitsky I. Principles of long noncoding rna evolution derived from direct comparison of transcriptomes in 17 species. *Cell reports*. 2015;11:1110-1122
18. Necsulea A, Soumillon M, Warnefors M, Liechti A, Daish T, Zeller U, Baker JC, Grutzner F, Kaessmann H. The evolution of lncrna repertoires and expression patterns in tetrapods. *Nature*. 2014;505:635-640
19. Ulitsky I, Shkumatava A, Jan CH, Sive H, Bartel DP. Conserved function of lincrnas in vertebrate embryonic development despite rapid sequence evolution. *Cell*. 2011;147:1537-1550
20. Lin J, Zhang X, Xue C, Zhang H, Shashaty MG, Gosai SJ, Meyer N, Grazioli A, Hinkle C, Caughey J, Li W, Susztak K, Gregory BD, Li M, Reilly MP. The long noncoding rna landscape in hypoxic and inflammatory renal epithelial injury. *American journal of physiology. Renal physiology*. 2015;309:F901-913
21. Camacho C, Coulouris G, Avagyan V, Ma N, Papadopoulos J, Bealer K, Madden TL. Blast+: Architecture and applications. *BMC bioinformatics*. 2009;10:421
22. Alvarez-Dominguez JR, Bai Z, Xu D, Yuan B, Lo KA, Yoon MJ, Lim YC, Knoll M, Slavov N, Chen S, Chen P, Lodish HF, Sun L. De novo reconstruction of adipose tissue transcriptomes reveals long non-coding rna regulators of brown adipocyte development. *Cell metabolism*. 2015;21:764-776
23. Saeed S, Quintin J, Kerstens HH, Rao NA, Aghajanirefah A, Matarese F, Cheng SC, Ratter J, Berentsen K, van der Ent MA, Sharifi N, Janssen-Megens EM, Ter Huurne M, Mandoli A, van Schaik T, Ng A, Burden F, Downes K, Frontini M, Kumar V, Giamarellos-Bourboulis EJ, Ouwehand WH, van der Meer JW, Joosten LA, Wijmenga C, Martens JH, Xavier RJ, Logie C, Netea MG, Stunnenberg HG. Epigenetic programming of monocyte-to-macrophage differentiation and trained innate immunity. *Science*. 2014;345:1251086
24. Pham TH, Benner C, Lichtinger M, Schwarzfischer L, Hu Y, Andreesen R, Chen W, Rehli M. Dynamic epigenetic enhancer signatures reveal key transcription factors associated with monocytic differentiation states. *Blood*. 2012;119:e161-171
25. Ramirez F, Dundar F, Diehl S, Gruning BA, Manke T. Deeptools: A flexible platform for exploring deep-sequencing data. *Nucleic acids research*. 2014;42:W187-191
26. Koch F, Fenouil R, Gut M, Cauchy P, Albert TK, Zacarias-Cabeza J, Spicuglia S, de la Chapelle AL, Heidemann M, Hintermair C, Eick D, Gut I, Ferrier P, Andrau JC. Transcription initiation platforms and gtf recruitment at tissue-specific enhancers and promoters. *Nature structural & molecular biology*. 2011;18:956-963
27. Welter D, MacArthur J, Morales J, Burdett T, Hall P, Junkins H, Klemm A, Flicek P, Manolio T, Hindorff L, Parkinson H. The nhgri gwas catalog, a curated resource of snp-trait associations. *Nucleic acids research*. 2014;42:D1001-1006
28. Altshuler DM, Gibbs RA, Peltonen L, Altshuler DM, Gibbs RA, Peltonen L, Dermitzakis E, Schaffner SF, Yu F, Peltonen L, Dermitzakis E, Bonnen PE, Altshuler DM, Gibbs RA, de Bakker PI, Deloukas P, Gabriel SB, Gwilliam R, Hunt S, Inouye M, Jia X, Palotie A, Parkin M, Whittaker P, Yu F, Chang K, Hawes A, Lewis LR, Ren Y, Wheeler D, Gibbs RA, Muzny DM, Barnes C, Darvishi K, Hurles M, Korn JM, Kristiansson K, Lee C, McCarrol SA, Nemesh J, Dermitzakis E, Keinan A, Montgomery SB, Pollack S, Price AL, Soranzo N, Bonnen PE, Gibbs RA, Gonzaga-Jauregui C, Keinan A, Price AL, Yu F, Anttila V, Brodeur W, Daly MJ, Leslie S, McVean G, Moutsianas L, Nguyen H, Schaffner SF, Zhang Q, Ghori MJ, McGinnis R, McLaren W, Pollack S, Price AL, Schaffner SF, Takeuchi F, Grossman SR, Shlyakhter I, Hostetter EB, Sabeti PC, Adebamowo CA, Foster MW, Gordon DR, Licinio J, Manca MC, Marshall PA, Matsuda I, Ngare D, Wang VO, Reddy D, Rotimi CN, Royal CD, Sharp RR, Zeng C, Brooks LD, McEwen JE. Integrating common and rare genetic variation in diverse human populations. *Nature*. 2010;467:52-58

29. Benjamini Y, Yekutieli D. The control of the false discovery rate in multiple testing under dependency. *Annals of Statistics*. 2001;29:1165–1188
30. Qian J, Nunez S, Reed E, Reilly MP, Foulkes AS. A simple test of class-level genetic association can reveal novel cardiometabolic trait loci. *PloS one*. 2016;11:e0148218
31. Abecasis GR, Auton A, Brooks LD, DePristo MA, Durbin RM, Handsaker RE, Kang HM, Marth GT, McVean GA. An integrated map of genetic variation from 1,092 human genomes. *Nature*. 2012;491:56-65
32. Benjamini Y, Hochberg Y. Controlling the false discovery rate: A practical and powerful approach to multiple testing. *Journal of the Royal Statistical Society. Series B (Methodological),* . 1995;57:289-300
33. Huang da W, Sherman BT, Lempicki RA. Systematic and integrative analysis of large gene lists using david bioinformatics resources. *Nature protocols*. 2009;4:44-57
34. Carpenter S, Aiello D, Atianand MK, Ricci EP, Gandhi P, Hall LL, Byron M, Monks B, Henry-Bezy M, Lawrence JB, O'Neill LA, Moore MJ, Caffrey DR, Fitzgerald KA. A long noncoding rna mediates both activation and repression of immune response genes. *Science*. 2013;341:789-792
35. Ostuni R, Piccolo V, Barozzi I, Polletti S, Termanini A, Bonifacio S, Curina A, Prosperini E, Ghisletti S, Natoli G. Latent enhancers activated by stimulation in differentiated cells. *Cell*. 2013;152:157-171
36. Squadrito ML, Baer C, Burdet F, Maderna C, Gilfillan GD, Lyle R, Ibberson M, De Palma M. Endogenous rnas modulate microrna sorting to exosomes and transfer to acceptor cells. *Cell reports*. 2014;8:1432-1446
37. Xue C, Zhang X, Zhang H, Ferguson JF, Wang Y, Hinkle C, Li M, Reilly MP. De novo rna sequence assembly during in vivo inflammatory stress reveals hundreds of unannotated lincrnas in human blood cd14+ monocytes and in adipose tissue. *Physiological genomics*. 2017:physiolgenomics.00001.02017